

Properties and baroclinic instability of stratified thermal upper-ocean flow

F.J. Beron-Vera
Department of Atmospheric Sciences
Rosenstiel School of Marine,
Atmospheric & Earth Science
University of Miami
Miami, Florida, USA
fberon@miami.edu

M.J. Olascoaga
Department of Ocean Sciences
Rosenstiel School of Marine,
Atmospheric & Earth Science
University of Miami
Miami, Florida, USA
jolascoaga@miami.edu

Submitted to *Proceedings of the Royal Society A*.
Started: October 27, 2023. This version: March 28, 2024.

Contents

1	Introduction	2
2	The $IL^{(0,1)}$QG	5
2.1	Model equations	6
2.2	Uniqueness of solutions	9
2.3	Circulations	9
2.3.1	A Kelvin circulation theorem	9
2.3.2	Circulation of the velocity	10
2.4	Invariant subspaces	11
2.5	Hamiltonian structure	11
2.6	Topographic forcing	14
2.7	Conservation laws	15
2.7.1	Energy, zonal momentum, and Casimirs	15
2.7.2	Non-Casimir, non-explicit-symmetry-related conservation laws . . .	17
3	Linear waves and free energy	18
4	Stability of baroclinic zonal flow	20
4.1	Spectral stability	21
4.2	Formal stability	26
4.3	Lyapunov stability	28

5	Nonlinear saturation of unstable baroclinic zonal flow	29
6	Discussion	30
7	Concluding remarks	33

Abstract

We study the properties of, and perform a stability analysis of a baroclinic zonal current in, a thermal rotating shallow-water model, sometimes called *Ripa's model*, featuring stratification for quasigeostrophic upper-ocean dynamics. The model has Lie–Poisson Hamiltonian structure. In addition to Casimirs, the model supports integrals of motion that neither form the kernel of the bracket nor are related to explicit symmetries. The model sustains Rossby waves and a neutral model, whose spurious growth is prevented by a positive-definite integral, quadratic on the deviation from the motionless state. A baroclinic zonal jet with vertical curvature is found to be spectrally stable for specific configurations of the gradients of layer thickness, vertically averaged buoyancy, and buoyancy frequency. Only a subset of such states was found Lyapunov stable using the available integrals, except the newly reported ones, whose role in constraining stratified thermal flow remains elusive. The existence of Lyapunov-stable states enabled bounding the nonlinear growth of perturbations to spectrally unstable states. Our results do not support the generality of earlier numerical evidence on the suppression of submesoscale wave activity as a result of the inclusion of stratification in thermal shallow-water theory, which we supported with direct numerical simulations.

On the occasion of the 50th anniversary of Departamento de Oceanografía Física of CICESE (Ensenada, Baja California, Mexico), we dedicate this paper to the memory of Pedro Ripa (1946–2001), who commended us to listen to the whispers in the woods.

Keywords Ocean mixed layer · Submesoscales · Thermal shallow water · Stratification · Noncanonical Hamiltonian structure · Conservation laws · Baroclinic instability · Arnold's method · Shepherd's method

1 Introduction

The uppermost part of the ocean, i.e., above the main thermocline including the mixed layer, is characterized by the ubiquitous presence of highly energetic mesoscale (20–300 km) eddies (vortices) with life spans of weeks to months which dominate horizontal transport and are important contributors to vertical transport with consequences for the overall biogeochemical cycle (e.g., [McG16] and references therein). In recent decades, high-resolution numerical simulations and field observations have revealed that vertical transport is also influenced by motions at submesoscales (1–10 km) in the form of Kelvin–Helmholtz-like vortices that roll up along density fronts (e.g., [Mah16] and references therein).

Mesoscale motions are well described by quasigeostrophic (QG) theory, valid, roughly speaking, for length scales of the order of the gravest baroclinic (i.e., internal) Rossby radius of deformation and time scales much longer than the inverse of the Coriolis parameter [Ped87]. The simplest QG model, capable to provide a minimal description of mesoscale upper-ocean flow, has a layer of constant density, limited from above by a rigid lid and from below by a soft interface with an infinitely deep layer of quiescent fluid. Using notation introduced by Ripa [Rip95], we will refer to this model as the *HLQG* for including a *homogeneous* (density) *layer*. Submesoscale motions, with smaller length scales and faster time scales than mesoscale motions, are, in principle, beyond the scope of QG theory [McW16]. However, based on numerical simulations, an interesting observation has been recently made [HHS22] that submesoscale motions can indeed be represented by a QG model with one layer when lateral inhomogeneity is allowed in the buoyancy (temperature) field. Such simulations revealed sub-deformation scale (i.e., submesoscale) vortex rolls akin to structures commonly observed in surface ocean color pictures acquired by satellites. A result of a simulation of that type as produced by ourselves along with an outstanding cloud-free ocean color image revealing submesoscale vortices are shown in Fig. 1.

The above kind of QG model, referred to as *thermal QG model* by [WD13], has a long history. It was derived by Ripa [Rip96b] asymptotically from the thermal primitive equations (PE) upon expanding them in small Rossby number. The thermal PE, or rotating shallow-water [WD13], model was introduced in the 1960s [OR67], widely employed from early the 1980s through the early 2000s (e.g., [SC83, MK88, FMP95]), particularly at CICESE (e.g., [Bei97, OSP98, PP00]), generalized to a system of multiple layers by Ripa [Rip93b], and investigated theoretically by him [Rip96a, Rip95, Rip99]. Due to Ripa’s several contributions, the thermal QG and PE models have been referred to as *Ripa’s models* [Del03]. Honoring notation introduced by [Rip95], we will refer to these models as models of the IL^0 class, where “IL” emphasizes that the models have a (stack of many) *inhomogeneous layer(s)* and the superscript indicates that their fields do not vary in the vertical.

In recent years the IL^0 has made a strong comeback [GLZD17, EDK19, LZD20, KLZ20, HHS22, ACBVG+22, CKLZ23, CHL+23], motivated in large part by the tendency of lateral temperature gradients in the upper ocean to become steeper as the ocean absorbs heat from a warming troposphere. In particular, [BV21c] introduced a family of IL-type models, both in PE and for QG dynamics, featuring stratification. The buoyancy field in this model family, referred to as $IL^{(0,n)}$, is written as a polynomial in the vertical coordinate of arbitrary whole degree (n) with coefficients that vary laterally and with time while they are advected (by Lie transport) under the flow of the model horizontal velocity, which is vertically uniform, assigning meaning to the first slot in the superscript in $IL^{(0,n)}$. The $IL^{(0,n)}$ PE models admit an Euler–Poincare variational formulation [HMR02] and, via a partial Legendre transform, possess a Lie–Poisson, i.e., noncanonical, Hamiltonian structure [MG80]. The $IL^{(0,n)}$ QG, derived asymptotically from the $IL^{(0,n)}$ PE, are Hamiltonian in a Lie–Poisson sense. Including stratification in the IL models expands their scope, for

instance, by enabling them to represent important processes such as the restratification of the mixed layer, which follows the development of submesoscale motions by baroclinic instability [BFF07]. (In an attempt to add more physics to the IL models, velocity vertical shear is included in [Rip95] in the single layer case and in [BV21a] in a system with multiple layers. However, the resulting IL models with stratification and vertical shear do not enjoy the aforementioned geometric mechanics properties.)

Goals of the paper. In this paper we investigate in some depth the properties of the recently proposed stratified IL models by focusing on the $IL^{(0,1)}QG$. We also study how the model fares with respect to baroclinic instability, which, as noted, is an important source of submesoscale circulatory motions in the ocean mixed layer.

It may sound awkward to attempt an investigation of baroclinic instability using an IL model involving a single layer since the (horizontal) velocity is vertically uniform. Two layers may seem to be required as is needed to represent baroclinic instability using the HLQG in the so-called Phillips problem [Ped87]. However, by the thermal-wind balance, which dominates at low frequency, in (every layer of) an IL model the velocity field *implicitly* includes shear in the vertical. Furthermore, implicitly, the velocity vertical profile in the $IL^{(0,1)}$ is curved. This extends the standard baroclinic instability problem of Phillips, or Eady in the continuously stratified case [Ped87], from uniform vertical shear (linear vertical profile) to velocity with vertical curvature, which augments the dimension of the space of parameters for exploration.

While the study of this paper is of interest per se, a motivation for pursuing it is found in numerical simulations presented in [BV21c]. These simulations have suggested that inclusion of stratification in the IL models tends to halt the development of submesoscale circulations. This followed from the comparison of evolutions in the IL^0QG and $IL^{(0,1)}QG$ forced by bottom topography, which can be included without spoiling the Hamiltonian structure of the models. (This was shown in [BV21b, HLP21] to hold for the IL^0QG and here we show that it also applies to the $IL^{(0,1)}QG$.) The study carried out here will help assess the generality of the numerical evidence presented in [BV21c].

Paper organization. The rest of the paper is organized as follows. In Section 2 we review the $IL^{(0,1)}QG$ and describe its properties. Specifically, Section 2.1 presents the model equations along with its boundary conditions and a physical interpretation of its variables. Section 2.2 discusses uniqueness of solution in the model. Section 2.3 is dedicated to discussing theorems of circulation, of an appropriately defined Kelvin–Noether-like quantity along material loops (Section 2.3.1) and of the velocity along solid boundaries of the flow domain (Section 2.3.2). Invariant subspaces of the model are considered in Section 2.4. In Section 2.5 the Lie–Poisson Hamiltonian structure is clarified, particularly in relation with boundary conditions, which were only superficially discussed in [BV21c]. Inclusion of topographic forcing without destroying Hamiltonian structure is treated in Section 2.6.

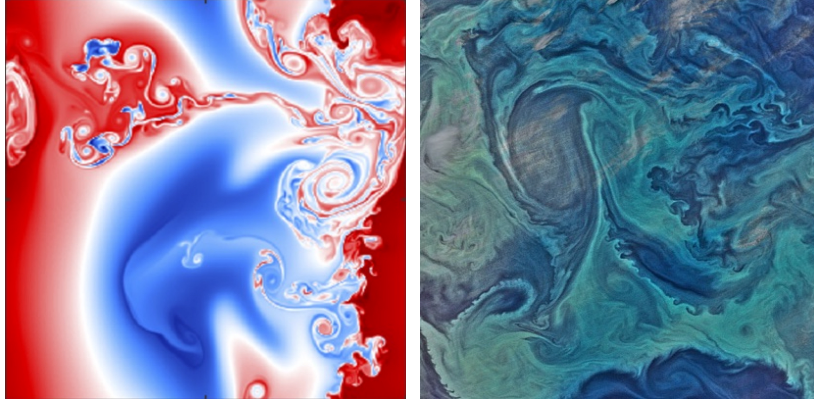


Figure 1: (left) Emergent cascade of submesoscale vorticity filament rollups in a reduced-gravity direct numerical simulation of the IL^0QG with topographic forcing in a doubly periodic domain $\mathbb{R}/R\mathbb{Z} \times \mathbb{R}/R\mathbb{Z}$ of the β -plane, where $R \approx 25$ km is the baroclinic Rossby radius of deformation. (right) Ocean color image acquired by VIIRS (Visible Infrared Imaging Radiometer Suite) on 1 January 2015 west of the Drake Passage in the Southern Ocean, revealing vortices with diameters ranging from a couple of km to a couple of hundred km. Image credit: NASA Ocean Color Web (<https://oceancolor.gsfc.nasa.gov/gallery/447/>).

Reviewing the Hamiltonian structure of the $\text{IL}^{(0,1)}\text{QG}$ is helpful for Section 2.7, which is devoted to describing the conservation laws of the system, which, when linked to explicit symmetries, are obtained via a Noether’s theorem appropriate for noncanonical Hamiltonian systems. The conservation laws include a newly reported family of integrals of motion that are neither link to explicit symmetries (via Noether’s theorem) nor form the kernel of the Lie–Poisson bracket of the system. Such motion integrals have, to the best of our knowledge, never been reported to date. Linear waves are discussed in Section 3. Section 4 is dedicated to investigate the stability of a baroclinic zonal flow on the β -plane with vertical curvature. Three types of stability notions are discussed, namely, spectral (Section 4.1), formal (Section 4.2), and Lyapunov (Section 4.3). In Section 5 we derive a-priori bounds on the nonlinear growth of perturbations to unstable basic states. A discussion, accompanied by direct numerical simulations, of differences between behavior in the $\text{IL}^{(0,1)}\text{QG}$ and IL^0QG is offered in Section 6. Section 7 presents the conclusions from the paper. Finally, an Appendix is included containing numerical details of the direct simulations.

2 The $\text{IL}^{(0,1)}\text{QG}$

Let $\mathbf{x} = (x, y)$ denote position on a periodic zonal domain $\mathcal{D} = \mathbb{R}/L\mathbb{Z} \times [0, W]$ of the β plane. That is, the channel rotates steadily at angular velocity $\frac{1}{2}f\hat{\mathbf{z}}$, where $f = f_0 + \beta y$ is the Coriolis parameter. We will denote by $\partial\mathcal{D}_-$ (resp., $\partial\mathcal{D}_+$) the southern (resp., northern)

wall of the channel at $y = 0$ (resp., $y = W$). Consider a layer of (ideal) fluid limited from above by a horizontally rigid lid at $z = 0$ and from below by a soft interface at $z = -h(\mathbf{x}, t)$ with an infinitely deep layer of homogeneous fluid at rest. As in (rotating) shallow-water theory, the motion in the active (top) layer is assumed to be columnar. The vertically shearless horizontal velocity is denoted by $\bar{\mathbf{u}}(\mathbf{x}, t)$, where the overbar represents a vertical average. As in standard *thermal* shallow-water theory, the active layer buoyancy is allowed to vary in horizontal position and time [Rip93b]. But unlike this theory, the buoyancy is allowed to vary in the vertical as well [BV21c]. In the $IL^{(0,1)}$ class of *stratified* thermal shallow-water models, of interest here, this is done by writing the buoyancy as

$$\vartheta(\mathbf{x}, z, t) = \bar{\vartheta}(\mathbf{x}, t) + \left(1 + \frac{2z}{h(\mathbf{x}, t)}\right) \vartheta_\sigma(\mathbf{x}, t). \quad (1)$$

That is, the stratification in the active layer is set to be uniform, with the buoyancy (linearly) varying from $\bar{\vartheta} + \vartheta_\sigma$ at $z = 0$ to $\bar{\vartheta} - \vartheta_\sigma$ at $z = -h$. This imposes the condition

$$\bar{\vartheta} \geq \vartheta_\sigma > 0, \quad (2)$$

stating that the buoyancy is everywhere positive and the density increases with depth. For future reference, we introduce the instantaneous buoyancy (or Brunt–Väisälä) frequency squared

$$n^2(\mathbf{x}, z, t) := \partial_z \vartheta(\mathbf{x}, z, t) = 2 \frac{\vartheta_\sigma(\mathbf{x}, t)}{h(\mathbf{x}, t)}. \quad (3)$$

Remark 1 (On notation). *The subscript notation is motivated by denoting by σ , as in [Rip95], the scaled vertical coordinate $1 + \frac{2z}{h(\mathbf{x}, t)}$. For instance, in the $IL^{(0,2)}$ model class [BV21c] the buoyancy is written as $\vartheta = \bar{\vartheta} + \sigma \vartheta_\sigma + (\sigma^2 - \frac{1}{3}) \vartheta_{\sigma^2}$, clarifying additional notation introduced below.*

2.1 Model equations

The evolution equations of the $IL^{(0,1)}$ QG in the reduced-gravity setting above are given by [BV21c]

$$\partial_t \bar{\xi} + \{\bar{\psi}, \bar{\xi} - R_S^{-2}(\psi_\sigma - \frac{2}{3}\psi_{\sigma^2})\}_{xy} = 0, \quad (4a)$$

$$\partial_t \psi_\sigma + \{\bar{\psi}, \psi_\sigma\}_{xy} = 0, \quad (4b)$$

$$\partial_t \psi_{\sigma^2} + \{\bar{\psi}, \psi_{\sigma^2}\}_{xy} = 0, \quad (4c)$$

where

$$\nabla^2 \bar{\psi} - R_S^{-2} \bar{\psi} = \bar{\xi} - R_S^{-2}(\psi_\sigma - \frac{2}{3}\psi_{\sigma^2}) - \beta y \quad (4d)$$

with

$$R_S^2 := (1 - \frac{1}{3}S) R^2. \quad (4e)$$

Here

$$\{a, b\}_{xy} := \nabla^\perp a \cdot \nabla b \quad (4f)$$

for any differentiable functions $a, b(\mathbf{x}, t)$, where ∇^\perp is short for $\hat{\mathbf{z}} \times \nabla$, is the Jacobian of the transformation $(x, y) \mapsto (a, b)$ and

$$R := \frac{\sqrt{g_r H_r}}{|f_0|}, \quad S := \frac{N_r^2 H_r}{2g_r}. \quad (4g)$$

The positive constants H_r , g_r , and N_r^2 are reference (i.e., in the absence of currents) layer thickness, vertically averaged buoyancy,¹ and buoyancy frequency squared, respectively. The (positive) constant on the left in (4g) corresponds to the equivalent barotropic (external) Rossby radius of deformation in a model with arbitrary stratification in a reduced-gravity setting. The constant on the right in (4g) is a measure of reference stratification. The reference buoyancy varies from $1 + S$ at $z = 0$ to $1 - S$ at $z = -H_r$. Thus, by static stability, $0 < S < 1$.

The system is subjected to

$$\nabla \bar{\psi} \times \hat{\mathbf{n}}|_{\partial \mathcal{D}_\pm} = 0 \iff \partial_x|_{y=0, W} \bar{\psi} = 0 \quad (5a)$$

and periodicity in the along channel direction, x , i.e.,

$$\bar{\xi}(x + L, y, t) = \bar{\xi}(x, y, t) \quad (5b)$$

and similarly for the rest of the variables.

The $\text{IL}^{(0,1)}\text{QG}$ has three prognostic fields, $(\bar{\xi}, \psi_\sigma, \psi_{\sigma^2})$, assumed to be sufficiently smooth in each of its arguments, (\mathbf{x}, t) . These diagnose $\bar{\psi}(\mathbf{x}, t)$ via (4d), which defines the invertibility principle for the $\text{IL}^{(0,1)}\text{QG}$. (In Fourier space, say, the positive-definite symmetric operator $R_S^{-2} - \nabla^2$ is nondegenerate; hence, its operator inverse $(R_S^{-2} - \nabla^2)^{-1}$ exists and is well defined.) The physical meaning of these variables is as follows. Let $\text{Ro} > 0$ be a small parameter taken to represent a Rossby number, measuring the strength of inertial and Coriolis forces, e.g.,

$$\text{Ro} = \frac{V}{|f_0|R} \ll 1, \quad (6)$$

where V is a characteristic velocity. In the QG scaling [Ped87]

$$(|\bar{\mathbf{u}}|, h - H_r, \partial_t, \beta y) = O(\text{Ro}V, \text{Ro}R, \text{Ro}f_0, \text{Ro}f_0). \quad (7)$$

Consistent with (7), with an $O(\text{Ro}^2)$ error,

$$\bar{\mathbf{u}} = \nabla^\perp \bar{\psi}, \quad (8)$$

¹In [BV21c], $2g_r$ is incorrectly referred to as the reference buoyancy jump at the bottom of the active layer.

$$h = H_r + \frac{H_r}{f_0 R_S^2} (\bar{\psi} - \psi_\sigma + \frac{2}{3} \psi_{\sigma^2}) \quad (9)$$

$$\bar{\vartheta} = g_r + \frac{2g_r}{f_0 R^2} \psi_\sigma, \quad (10)$$

$$\vartheta_\sigma = \frac{1}{2} N_r^2 H_r + \frac{4g_r}{f_0 R^2} \psi_{\sigma^2}, \quad (11)$$

where

$$\frac{\psi_\sigma - 2\psi_{\sigma^2}}{f_0 R^2} \geq \frac{S-1}{2}, \quad \frac{\psi_{\sigma^2}}{f_0 R^2} > -\frac{S}{4}, \quad (12)$$

by (2). Finally, with an $O(\text{Ro}^2)$ error,

$$\frac{\nabla^\perp \cdot \bar{\mathbf{u}} + f}{h} = \frac{f_0 + \bar{\xi}}{H_r}. \quad (13)$$

The left-hand-side of (13) is proportional to the Ertel $\frac{z}{h}$ -potential vorticity in the hydrostatic approximation and with the horizontal velocity replaced with $\bar{\mathbf{u}}$ [cf. Rip95, for details]. Thus $\bar{\xi}$ can be identified with potential vorticity in the $\text{IL}^{(0,1)}\text{QG}$.

With the identifications (8)–(13), equation (4a) controls the evolution of $\text{IL}^{(0,1)}\text{QG}$ potential vorticity. This quantity is not materially conserved, i.e., advected (by Lie transport) under the flow of $\nabla^\perp \bar{\psi}$. Rather, the potential vorticity in the $\text{IL}^{(0,1)}\text{QG}$ is created (or annihilated) by the presence of buoyancy gradients (cf. Section 2.3.1, for additional discussion). This is consistent with Ertel’s $\frac{z}{h}$ -potential vorticity not being materially conserved. Equations (43b) and (43c) control, respectively, the evolution of the vertical average and gradient of buoyancy. These are both materially conserved. Altogether (43b) and (43c) give material conservation of buoyancy in the $\text{IL}^{(0,1)}\text{QG}$. Finally, the boundary condition (5a) means no flow through the solid walls of the zonal channel domain.

Remark 2 (Implicit vertical shear). *By the thermal-wind balance, the velocity has implicit vertical curvature, which motivates the streamfunction notations ψ_σ and ψ_{σ^2} [BV21c]. Indeed, the buoyancy distribution (1) implicitly implies that the velocity is determined, with an $O(\text{Ro}^2)$ error, by the streamfunction*

$$\psi = \bar{\psi} + \left(1 + \frac{2z}{H_r}\right) \psi_\sigma + \left(\left(1 + \frac{2z}{H_r}\right)^2 - \frac{1}{3}\right) \psi_{\sigma^2}. \quad (14)$$

We note that the IL^0QG can be recovered from system (43) upon omitting ψ_{σ^2} and setting $S = 0$, i.e., replacing R_S with R . Note, for instance, that the buoyancy restriction in the IL^0QG is $\psi_\sigma > -\frac{1}{2}f_0 R^2$. The potential vorticity in the IL^0QG , given by $\bar{\xi} = \nabla^2 \bar{\psi} - R^{-2}(\bar{\psi} - \psi_\sigma) + \beta y$, is created (or annihilated) as in the $\text{IL}^{(0,1)}\text{QG}$ due to lateral changes in buoyancy, which is only permitted to vary in the horizontal (and time). This is unlike the HLQG , which follows from the IL^0QG after ignoring ψ_σ . The potential vorticity

in the HLQG, $\bar{\xi} = \nabla^2 \bar{\psi} - R^{-2} \bar{\psi} + \beta y$, is materially conserved. The results discussed below for the IL^(0,1)QG can be translated to corresponding results for the IL⁰QG or HLQG in the indicated limits.

2.2 Uniqueness of solutions

Assume that $\bar{\psi}_1(\mathbf{x}, t)$ and $\bar{\psi}_2(\mathbf{x}, t)$ are two solutions of (4d), on the zonal channel domain \mathcal{D} , each one satisfying boundary conditions (5). Let $\phi := \bar{\psi}_1 - \bar{\psi}_2$; then

$$\nabla^2 \phi - R_S^{-2} \phi = 0 \quad (15)$$

on \mathcal{D} subjected to

$$\nabla \phi \times \hat{\mathbf{n}}|_{\partial \mathcal{D}_{\pm}} = 0 \iff \partial_x|_{y=0, W} \phi = 0, \quad \phi(x, 0, t) = \phi(x, L, t). \quad (16)$$

Multiplying (15) by ϕ and integrating by parts with (16) in mind,

$$\int_{\mathcal{D}} |\nabla \phi|^2 + R_S^{-2} \phi^2 d^2x = 0, \quad (17)$$

which holds if and only if $\phi = 0$, i.e., $\psi_1 = \psi_2$.

2.3 Circulations

2.3.1 A Kelvin circulation theorem

Let

$$\mathbf{u}_{\sigma} := \nabla^{\perp} \psi_{\sigma}, \quad \mathbf{u}_{\sigma^2} := \nabla^{\perp} \psi_{\sigma^2}. \quad (18)$$

Let $\mathbf{f}(\mathbf{x})$ be the vector potential of the Coriolis parameter, viz., $f_0 + \beta y = \nabla^{\perp} \cdot \mathbf{f}$. Let in addition $\partial \mathcal{D}_t$ be the material loop enclosing a material region \mathcal{D}_t , i.e., advected by the flow of $\bar{\mathbf{u}}$. Consider

$$\mathcal{K} := \oint_{\partial \mathcal{D}_t} (\bar{\mathbf{u}} + \mathbf{f} - R_S^{-2} \nabla^{-2} (\bar{\mathbf{u}} - \mathbf{u}_{\sigma} + \mathbf{u}_{\sigma^2})) \cdot d\mathbf{x} = \int_{\mathcal{D}_t} \bar{\xi} d^2x, \quad (19)$$

where the last equality follows upon using Stokes' theorem and holds with an $O(\text{Ro}^2)$ error. The above is an appropriate definition of the Kelvin circulation for the IL^(0,1)QG as it leads to a theorem analogous to the Kelvin–Noether theorem for the IL^(0,1)PE [BV21c]. It extends that one found in Sec. 3.1 of [Hol15] for adiabatic QG dynamics to stratified thermal QG dynamics. By (4a) and after pulling back the integrand in the last equality of (19) and changing variables, it follows that

$$\dot{\mathcal{K}} = R_S^{-2} \int_{\mathcal{D}_t} \left\{ \bar{\psi}, \psi_{\sigma} - \frac{2}{3} \psi_{\sigma^2} \right\}_{xy} d^2x. \quad (20)$$

As in the $IL^{(0,1)}$ PE, the misalignment between the gradients of bathymetry and buoyancy creates (or destroys) Kelvin circulation. This is most cleanly seen by noting that

$$\int_{\mathcal{D}_t} \nabla^\perp h \cdot \nabla \left(\bar{\vartheta} - \frac{1}{3} \vartheta_\sigma \right) d^2x = 2R_S^{-2} \int_{\mathcal{D}_t} \{ \bar{\psi}, \psi_\sigma - \frac{2}{3} \psi_{\sigma^2} \}_{xy} d^2x \quad (21)$$

with an $O(\text{Ro}^3)$ error.

Remark 3. *Two exceptions are as follows.*

1. Note that $\{ \bar{\psi}, \psi_\sigma - \frac{2}{3} \psi_{\sigma^2} \}_{xy} = \nabla^\perp \bar{\psi} \cdot \nabla (\psi_\sigma - \frac{2}{3} \psi_{\sigma^2}) = -\nabla \bar{\psi} \cdot \nabla^\perp (\psi_\sigma - \frac{2}{3} \psi_{\sigma^2})$. Since $\nabla \cdot \nabla^\perp = 0$, then by Stokes' theorem the integral on the right-hand-side of (20) is equal to $-\oint_{\partial \mathcal{D}_t} \bar{\psi} \nabla^\perp (\psi_\sigma - \frac{2}{3} \psi_{\sigma^2}) \cdot \hat{\mathbf{n}} ds$. This vanishes if ψ_σ and ψ_{σ^2} are constant along \mathcal{D}_t . The Kelvin circulation is conserved in these circumstances, which express that the material loop $\partial \mathcal{D}_t$ is isopycnic at each level in the vertical.
2. When \mathcal{D}_t is replaced by the zonal channel domain \mathcal{D} , then the Kelvin circulation is conserved, whether $\partial \mathcal{D}$ is levelwise isopycnic or not. To see this, first note that, in such a case, the integral on right-hand-side of (20) is replaced by $\int_{\mathcal{D}} \{ \bar{\psi}, R_S^{-2} (\psi_\sigma - \frac{2}{3} \psi_{\sigma^2}) - \bar{\xi} \}_{xy} d^2x$. By (5b) this is equal to $(\int_{\partial \mathcal{D}_-} - \int_{\partial \mathcal{D}_+}) (R_S^{-2} (\psi_\sigma - \frac{2}{3} \psi_{\sigma^2}) - \bar{\xi}) \nabla^\perp \bar{\psi} \cdot \hat{\mathbf{n}} ds$, upon invoking Stokes' theorem. By (5b) each term of this sum individually vanishes. This is unlike the $IL^{(0,1)}$ PE, in which case $\partial \mathcal{D}_\pm$ must be levelwise isopycnic, making the $IL^{(0,1)}$ QG less restrictive than the $IL^{(0,1)}$ PE. (In that model and the present one, if this condition is imposed initially, then it is preserved for all time.)

2.3.2 Circulation of the velocity

Consider

$$\gamma_\pm := \int_{\partial \mathcal{D}_\pm} \nabla \bar{\psi} \cdot \hat{\mathbf{n}} ds, \quad (22)$$

defining the circulations of the velocity along the coasts of the zonal channel domain. Note the difference with the circulation integral, which we have referred to as a Kelvin circulation for QG, in the preceding section. We will impose the condition

$$\dot{\gamma}_\pm = 0. \quad (23)$$

Constancy of γ_\pm is a boundary condition, in addition to (5), which guarantees energy preservation (cf. Section 2.7.1). This is not a peculiarity of the $IL^{(0,1)}$ QG, but a rather general aspect of QG models.

We note that when \mathcal{D} is replaced by \mathcal{D}_t in the definition of the Kelvin circulation (19), one has the relationship

$$\mathcal{K} = \bar{\psi}|_{\partial \mathcal{D}_-} \gamma_- + \bar{\psi}|_{\partial \mathcal{D}_+} \gamma_+ + \int_{\mathcal{D}} \beta y - R_S^{-2} (\bar{\psi} - \psi_\sigma + \frac{2}{3} \psi_{\sigma^2}) d^2x, \quad (24)$$

as it follows by using (4d). By Remark 3, it follows that

$$\frac{d}{dt} \int_{\mathcal{D}} \bar{\psi} d^2x = 0. \quad (25)$$

This result may be seen to express volume preservation with an $O(\text{Ro}^3)$ error. Indeed, one may deduce this result by starting from the advection equation of hd^2x or local volume conservation law in the $\text{IL}^{(0,1)}\text{PE}$, viz., $\partial_t h + \nabla \cdot h \bar{\mathbf{u}} = 0$. Then one may use (9) and apply the QG asymptotic expansion taking into account that, in the $\text{IL}^{(0,1)}\text{PE}$, $\bar{\vartheta}$ and ϑ_σ are materially conserved. That is, $\bar{\vartheta}$ and ϑ_σ represent advected scalar quantities, evolving therefore as $\partial_t \bar{\vartheta} + \bar{\mathbf{u}} \cdot \nabla \bar{\vartheta} = 0$ and $\partial_t \vartheta_\sigma + \bar{\mathbf{u}} \cdot \nabla \vartheta_\sigma = 0$, respectively. However, nothing of this is available explicitly in the QG limit. In other words, (23) cannot be deduced from (25) by working with the $\text{IL}^{(0,1)}\text{QG}$ model equations (4).

2.4 Invariant subspaces

If system (4) is initialized from $\psi_\sigma, \psi_{\sigma^2} = \text{const}$, then these variables preserve their initial constant values all the times. In other words, the subspace $\{\psi_\sigma, \psi_{\sigma^2} = \text{const}\}$ is an invariant subspace of the $\text{IL}^{(0,1)}\text{QG}$. The dynamics on this invariant subspace are formally the same as those in the adiabatic case, that is, the HLQG, in which case the potential vorticity, given by $\bar{\xi} = \nabla^2 \bar{\psi} - R^{-2} \bar{\psi} + \beta y$, is materially conserved. This holds formally because ψ_{σ^2} actually is a perturbation on a reference uniform stratification. But this is reflected in (4) only through the stratification parameter S . The HLQG and $\text{IL}^{(0,1)}\text{QG}$ potential vorticities on $\{\psi_\sigma, \psi_{\sigma^2} = \text{const}\}$ differ by unimportant constants and by the Rossby radius of deformation being smaller for $S \neq 0$. In turn, if (4) is initialized from $\psi_{\sigma^2} = \text{const}$, then this is preserved for all time. The dynamics on this invariant subspace is formally the same as that of the $\text{IL}^{(0,1)}\text{QG}$, with the caveats noted above. Similarly, in the $\text{IL}^{(0,1)}\text{QG}$, obtained from the $\text{IL}^{(0,1)}\text{QG}$ by ignoring ψ_{σ^2} and setting $S = 0$, the subspace $\{\psi_\sigma = \text{const}\}$ is invariant and on this invariant subspace the dynamics coincides with that of the HLQG, exactly in this case.

2.5 Hamiltonian structure

We begin with a definition that is helpful to understand operations in the rest of the paper. This is followed by an assumption, which enables us to frame the Hamiltonian structure of the $\text{IL}^{(0,1)}\text{QG}$ in a domain with boundaries consistent with the aforementioned definition.

Definition 1 (Functional, functional derivatives, and variations). *A functional \mathcal{F} of scalar fields $\varphi^j(\mathbf{x}, t)$, $j = 1, \dots, J$, denoted $\mathcal{F}[\varphi]$, is a map from a vector space V to \mathbb{R} . The functional derivatives of \mathcal{F} are defined as the unique elements $\frac{\delta}{\delta \varphi^j} \mathcal{F}$, $j = 1, \dots, J$, satisfying*

$$\left. \frac{d}{d\varepsilon} \right|_{\varepsilon=0} \mathcal{F}[\varphi + \varepsilon \delta \varphi] =: \sum_{j=1}^J \int_{\mathcal{D}} \frac{\delta \mathcal{F}}{\delta \varphi^j} \delta \varphi^j d^2x =: \delta \mathcal{F}[\delta \varphi; \varphi], \quad (26)$$

where ε is a real parameter and $\delta\varphi$ is called the variation of φ . The functional $\delta\mathcal{F}$, linear in $\delta\varphi$, is called the first variation of \mathcal{F} . The above is the Gateaux definition of functional derivative, which does not require V to be normed. However, it is convenient to be taken as such and furthermore complete (i.e., Banach), so contributions of the first and higher-order variations to the total variation can be measured. More specifically, the second variation of \mathcal{F} , quadratic in $\delta\varphi$,

$$\delta^2\mathcal{F}[\delta\varphi; \varphi] := \left. \frac{d^2}{d\varepsilon^2} \right|_{\varepsilon=0} \mathcal{F}[\varphi + \varepsilon\delta\varphi] =: \sum_{j,k=1}^J \int_{\mathcal{D}} \frac{\delta^2\mathcal{F}}{\delta\varphi^j \delta\varphi^k} \delta\varphi^j \delta\varphi^k d^2x, \quad (27)$$

where $\frac{\delta^2}{\delta\varphi^j \delta\varphi^k} \mathcal{F}$, $i, k = 1, \dots, J$, define the second functional derivatives of \mathcal{F} . Higher-order variations, as well as functional derivatives, are similarly defined, so that the total variation of \mathcal{F} ,

$$\Delta\mathcal{F}[\delta\varphi; \varphi] := \mathcal{F}[\varphi + \delta\varphi] - \mathcal{F}[\varphi] = \delta\mathcal{F}[\delta\varphi; \varphi] + \frac{1}{2!}\delta^2\mathcal{F}[\delta\varphi; \varphi] + \frac{1}{3!}\delta^3\mathcal{F}[\delta\varphi; \varphi] + \dots, \quad (28)$$

which is noted for future reference.

Assumption 1. We will assume that all variations in the sense of Definition 1 are restricted to those that preserve the circulation of the velocity along each wall of the zonal channel domain, namely,

$$\delta\gamma_{\pm} = 0. \quad (29)$$

The restriction (29) enables a Hamiltonian formulation of the $IL^{(0,1)}QG$ wherein variational calculus is consistent with Definition 1. Otherwise, the space variables must be augmented to include γ_{\pm} as done in [HMRW85]. However, this requires one to define the notion of variational derivative differently than in Definition 1 [LMM86].

Remark 4. While allowing variations of γ_{\pm} adds generality to the Hamiltonian formulation of the $IL^{(0,1)}QG$, the practical consequences of such added generality are minimal. This is illustrated in [Rip93a] for the stability problem.

Let

$$\mathcal{E}[\bar{\xi}, \psi_{\sigma}, \psi_{\sigma^2}] := \frac{1}{2} \int_{\mathcal{D}} |\nabla \bar{\psi}|^2 + R_S^{-2} \bar{\psi}^2 d^2x = -\frac{1}{2} \int_{\mathcal{D}} \bar{\psi} \left(\bar{\xi} - R_S^{-2} (\psi_{\sigma} - \frac{2}{3}\psi_{\sigma^2}) - \beta y \right) d^2x \quad (30)$$

be the energy, where the equality follows from (5) upon integration by parts. That \mathcal{E} indeed is a functional of $(\bar{\xi}, \psi_{\sigma}, \psi_{\sigma^2})$ follows by noting that

$$\bar{\psi} = (\nabla^2 - R_S^{-2})^{-1} (\bar{\xi} - R_S^{-2} (\psi_{\sigma} - \frac{2}{3}\psi_{\sigma^2}) - \beta y), \quad (31)$$

where $(\nabla^2 - R_S^{-2})^{-1}$ is interpreted in terms of the relevant Green's function of the elliptic problem (4d).

Now, consider

$$\begin{aligned} \{\mathcal{F}, \mathcal{G}\}[\bar{\xi}, \psi_\sigma, \psi_{\sigma^2}] &:= \int_{\mathcal{D}} \begin{pmatrix} \frac{\delta \mathcal{F}}{\delta \bar{\xi}} \\ \frac{\delta \mathcal{F}}{\delta \psi_\sigma} \\ \frac{\delta \mathcal{F}}{\delta \psi_{\sigma^2}} \end{pmatrix}^\top \begin{pmatrix} -[\bar{\xi}, \cdot] & -[\psi_\sigma, \cdot] & -[\psi_{\sigma^2}, \cdot] \\ -[\psi_\sigma, \cdot] & 0 & 0 \\ -[\psi_{\sigma^2}, \cdot] & 0 & 0 \end{pmatrix} \begin{pmatrix} \frac{\delta \mathcal{G}}{\delta \bar{\xi}} \\ \frac{\delta \mathcal{G}}{\delta \psi_\sigma} \\ \frac{\delta \mathcal{G}}{\delta \psi_{\sigma^2}} \end{pmatrix} d^2x \\ &= \int_{\mathcal{D}} \bar{\xi} \left\{ \frac{\delta \mathcal{F}}{\delta \bar{\xi}}, \frac{\delta \mathcal{G}}{\delta \bar{\xi}} \right\}_{xy} + \sum_{n=1}^2 \psi_{\sigma^n} \left(\left\{ \frac{\delta \mathcal{F}}{\delta \bar{\xi}}, \frac{\delta \mathcal{G}}{\delta \psi_{\sigma^n}} \right\}_{xy} + \left\{ \frac{\delta \mathcal{F}}{\delta \psi_{\sigma^n}}, \frac{\delta \mathcal{G}}{\delta \bar{\xi}} \right\}_{xy} \right) d^2x \end{aligned} \quad (32)$$

for any $\mathcal{F}, \mathcal{G}[\bar{\xi}, \psi_\sigma, \psi_{\sigma^2}]$, where the second equality follows upon integrating parts and requiring

$$\nabla \frac{\delta \mathcal{F}}{\delta \bar{\xi}} \times \hat{\mathbf{n}}|_{\partial \mathcal{D}_\pm} = 0, \quad \nabla \frac{\delta \mathcal{F}}{\delta \psi_\sigma} \times \hat{\mathbf{n}}|_{\partial \mathcal{D}_\pm} = 0, \quad \nabla \frac{\delta \mathcal{F}}{\delta \psi_{\sigma^2}} \times \hat{\mathbf{n}}|_{\partial \mathcal{D}_\pm} = 0, \quad (33)$$

for all $\mathcal{F}[\bar{\xi}, \psi_\sigma, \psi_{\sigma^2}]$.

Remark 5 (Admissible functionals). *Functionals satisfying (33) are referred to as admissible functionals [MS87]. If boundary conditions (33) are not imposed, then an appropriate redefinition of the functional derivative is needed for the second equality in (32) to hold, yet not without the imposition of some condition on the boundary terms; cf. [LMM86].*

For all $\mathcal{F}, \mathcal{G}, \mathcal{H}[\bar{\xi}, \psi_\sigma, \psi_{\sigma^2}]$, the bracket defined in (32) satisfies: $\{\mathcal{F} + \mathcal{G}, \mathcal{H}\} = \{\mathcal{F}, \mathcal{H}\} + \{\mathcal{G}, \mathcal{H}\}$ (bilinearity); $\{\mathcal{F}, \mathcal{G}\} = -\{\mathcal{G}, \mathcal{F}\}$ (antisymmetry); $\{\{\mathcal{F}, \mathcal{G}\}, \mathcal{H}\} + \{\{\mathcal{F}, \mathcal{H}\}, \mathcal{G}\} + \{\{\mathcal{G}, \mathcal{H}\}, \mathcal{F}\} = 0$ (Jacobi identity); and $\{\mathcal{F}\mathcal{G}, \mathcal{H}\} = \mathcal{F}\{\mathcal{G}, \mathcal{H}\} + \{\mathcal{F}, \mathcal{H}\}\mathcal{G}$ (Leibniz rule). These properties make $\{, \}$ a Poisson bracket and by its linear dependence on $(\bar{\xi}, \psi_\sigma, \psi_{\sigma^2})$ it is classified as of Lie–Poisson type. Such noncanonical brackets inherit the properties above from analogous properties of $\{, \}_{xy}$, the canonical bracket in \mathbb{R}^2 .

Since

$$\delta \mathcal{E} = - \int_{\mathcal{D}} \bar{\psi} \delta \bar{\xi} + R_S^{-2} \bar{\psi} \delta \psi_\sigma + \frac{2}{3} R_S^{-2} \bar{\psi} \delta \psi_{\sigma^2} d^2x, \quad (34)$$

where the boundary terms have cancelled out by Assumption 1, it follows that

$$\frac{\delta \mathcal{E}}{\delta \bar{\xi}} = -\bar{\psi}, \quad \frac{\delta \mathcal{E}}{\delta \psi_\sigma} = -R_S^{-2} \bar{\psi}, \quad \frac{\delta \mathcal{E}}{\delta \psi_{\sigma^2}} = -\frac{2}{3} R_S^{-2} \bar{\psi}. \quad (35)$$

Equations (4a)–(4b) then follow as

$$\partial_t \bar{\xi} = \{\bar{\xi}, \mathcal{E}\}, \quad \partial_t \psi_\sigma = \{\psi_\sigma, \mathcal{E}\}, \quad \partial_t \psi_{\sigma^2} = \{\psi_{\sigma^2}, \mathcal{E}\}. \quad (36)$$

In other words, the $\text{IL}^{(0,1)}\text{QG}$ model constitutes a Lie–Poisson Hamiltonian system in the variables $(\bar{\xi}, \psi_\sigma, \psi_{\sigma^2})$ with Hamiltonian given by (30) and Lie–Poisson bracket defined by (32). More generally, one has

$$\frac{d\mathcal{F}}{dt} = \{\mathcal{F}, \mathcal{E}\} \quad (37)$$

for all $\mathcal{F}[\bar{\xi}, \psi_\sigma, \psi_{\sigma^2}]$.

The IL^0QG is also Lie–Poisson Hamiltonian, with Hamiltonian given by (30) with R_S replaced by R and Lie–Poisson bracket given by (32) with ψ_{σ^2} ignored. The resulting bracket is a particular version of the one derived by Ripa [Rip96b] for a system more general than the IL^0QG . A (Lie–Poisson) deformation of the IL^0QG bracket, i.e., with the same kernel, appears in [HL21]. Interestingly, low- β magnetohydrodynamics [MH84] and incompressible, nonhydrostatic, Boussinesq fluid dynamics on a vertical plane share this bracket [Ben84].

Remark 6 (Geometric mechanics interpretation). *Geometric mechanics views ideal fluid motion on a fluid container \mathcal{D} , such as the zonal channel domain of interest here, as a mapping of initial conditions at time $t = 0$, regarded as labels taking values on \mathcal{D} , or configuration manifold, which is acted upon by the Lie group of diffeomorphisms [MRW84]. This way motion on \mathcal{D} is lifted to the group and identified with a curve on the group, whose left action on \mathcal{D} produces the fluid trajectories. The tangent lift of the velocity on \mathcal{D} is given by the action of the group on the right. This lives on the tangent space to the group at the identity, arranged to happen at $t = 0$. This represents a vector space, which together with a binary operation, namely, the Lie bracket, forms the Lie algebra of the group. The relevant Lie algebra for $\text{IL}^{(0,1)}\text{QG}$ dynamics is $\mathfrak{sdiff}(\mathcal{D})$, that is, the Lie algebra of the Lie group $\text{SDiff}(\mathcal{D})$ of area preserving diffeomorphisms of the zonal channel domain \mathcal{D} . The corresponding vector space is that of smooth time-dependent functions in \mathcal{D} , $C^\infty(\mathcal{D})$, and the Lie bracket is given by the canonical Poisson bracket, $\{, \}_{xy}$, given in (4f). Since $\{, \}_{xy}$ satisfies the Leibniz rule, $\mathfrak{sdiff}(\mathcal{D})$ is said to be a Lie enveloping algebra. The Lie–Poisson bracket (32) represents a product for a realization of a Lie enveloping algebra on functionals in the dual (with respect to the L^2 inner product) of $\mathfrak{sdiff}(\mathcal{D}) \ltimes (C^\infty(\mathcal{D}) \times C^\infty(\mathcal{D}))$, that is, the extension of $\mathfrak{sdiff}(\mathcal{D})$ by semidirect product to the vector space $\mathfrak{sdiff}(\mathcal{D}) \times C^\infty(\mathcal{D}) \times C^\infty(\mathcal{D})$ with the representation of $\mathfrak{sdiff}(\mathcal{D})$ on $C^\infty(\mathcal{D})$ given by $\{, \}_{xy}$.*

2.6 Topographic forcing

Let $\psi_0(\mathbf{x})$ be an arbitrary scalar function on the zonal channel domain \mathcal{D} of length-squared-over-time units, conveniently assumed to satisfy $\nabla\psi_0 \times \hat{\mathbf{n}}|_{\partial\mathcal{D}} = 0$. Let $L_0 = \text{const}$ have units of length. The Lie–Poisson Hamiltonian structure of the $\text{IL}^{(0,1)}\text{QG}$ is not spoiled if (43a) is modified as

$$\partial_t \bar{\xi} + \{\bar{\psi}, \bar{\xi} - R_S^{-2}(\psi_\sigma - \frac{2}{3}\psi_{\sigma^2})\}_{xy} = L_0^{-2}\{\psi_0, \psi_\sigma - \frac{2}{3}\psi_{\sigma^2}\}_{xy}, \quad (38)$$

which may be viewed as a topographic forcing to $\bar{\xi}$. System (43) with (43a) replaced with (38) is obtained from the Lie–Poisson bracket (32) with the Hamiltonian given by

$$\mathcal{E}[\bar{\xi}, \psi_\sigma, \psi_{\sigma^2}] := \frac{1}{2} \int_{\mathcal{D}} |\nabla \bar{\psi}|^2 + R_S^{-2} \bar{\psi}^2 - 2L_0^{-2} \psi_0 (\psi_\sigma - \frac{2}{3} \psi_{\sigma^2}) d^2x. \quad (39)$$

The change of the Kelvin circulation \mathcal{K} along a material loop $\partial\mathcal{D}_t$ is given now by $\int_{\mathcal{D}_t} [R_S^{-2} \bar{\psi} + L_0^{-2} \psi_0, \psi_\sigma - \frac{2}{3} \psi_{\sigma^2}] d^2x$ (cf. Section 2.3.1). As in the unforced case, \mathcal{K} is conserved when $\partial\mathcal{D}_t$ is levelwise isopycnic and along the walls $\partial\mathcal{D}_\pm$ of \mathcal{D} .

2.7 Conservation laws

2.7.1 Energy, zonal momentum, and Casimirs

The noncanonical Hamiltonian formalism allows conservation laws to be linked with symmetries via a form of *Noether's theorem*. A singular statement, due to Ripa [Rip92], is as follows.

Theorem 1 (Noether for noncanonical Hamiltonians). *Let P be a Poisson manifold, i.e., an infinite-dimensional smooth manifold endowed with a Poisson bracket or structure $\{, \} : C^\infty(P) \times C^\infty(P) \rightarrow C^\infty(P)$. The evolution of any functional $\mathcal{F}[\varphi] \in C^\infty(P) : P \rightarrow \mathbb{R}$ is controlled by (37) where $\mathcal{E}[\varphi]$ is a Hamiltonian. Consider the one-parameter family of variations induced by \mathcal{F} defined by $\delta_{\mathcal{F}} := \varepsilon \{ \mathcal{F}, \cdot \}$, where $\varepsilon > 0$ is small. The change induced by \mathcal{F} on another functional $\mathcal{G}[\varphi]$ is $\Delta_{\mathcal{F}} \mathcal{G} := \mathcal{G}[\varphi + \delta_{\mathcal{F}} \varphi] - \mathcal{G}[\varphi] = \varepsilon \{ \mathcal{G}, \mathcal{F} \}$ with an $O(\varepsilon^2)$ error. Moreover, with an $O(\varepsilon^2)$ error,*

$$\frac{d}{dt} \Delta_{\mathcal{F}} \mathcal{G} - \Delta_{\mathcal{F}} \frac{d\mathcal{G}}{dt} = \varepsilon \left\{ \frac{d\mathcal{G}}{dt}, \frac{d\mathcal{F}}{dt} \right\}. \quad (40)$$

Now, if $\frac{d}{dt} \mathcal{F} = 0$, i.e., \mathcal{F} is an integral of motion, then the infinitesimal transformation generated by \mathcal{F} is invariant under the dynamics, i.e., it represents a symmetry in the very general sense that making a transformation and letting the time run commute.

Remark 7. *The Poisson manifold P for the $IL^{(0,1)}QG$ is given by the geometric dual of $\mathfrak{sdiff}(\mathcal{D}) \times C^\infty(\mathcal{D}) \times C^\infty(\mathcal{D})$; cf. Remark 6.*

As noted by [Rip92], the reciprocal of the above theorem is, however, not strictly true. Indeed, if the left-hand-side of (40) vanishes, then $\frac{d}{dt} \mathcal{F} = 0$ is equal to a *distinguished function*. Namely, a function of functionals $\mathcal{C}[\varphi]$, called *Casimirs*, which are nontrivial solutions of

$$\{ \mathcal{F}, \mathcal{C} \} = 0 \forall \mathcal{F}. \quad (41)$$

The Casimirs form the kernel of $\{, \}$ and by (37) they are integrals of motion. However, they do not generate any variation, i.e., $\delta_{\mathcal{C}} \varphi = -\varepsilon \{ \mathcal{C}, \varphi \} = 0$, and thus are not related to

explicit symmetries, i.e., symmetries that are visible in the Eulerian variables that form the phase space in which the dynamics are being viewed.

With all the above in mind, take $\varphi = (\bar{\xi}, \psi_\sigma, \psi_{\sigma^2})$ and assume that \mathcal{F} is the generator of an infinitesimal time shift, namely, $t \rightarrow t - \varepsilon$, then $\delta_{\mathcal{F}}\varphi = -\varepsilon\partial_t\varphi$. The corresponding invariant is obtained by solving $-\partial_t\varphi = \{\varphi, \mathcal{F}\}$, which gives $\mathcal{F} = -\mathcal{E}$ (modulo a Casimir). Now suppose that \mathcal{E} is invariant under an infinitesimal translation in space, e.g., $x \rightarrow x - \varepsilon$. Then $\delta_{\mathcal{F}}\varphi = -\varepsilon\partial_x\varphi$. The corresponding invariant is the zonal (x) momentum \mathcal{M} , which is obtained (modulo a Casimir) by solving $-\partial_x\varphi = \{\varphi, \mathcal{M}\}$. This is readily seen to be given by

$$\mathcal{M}[\bar{\xi}, \psi_\sigma, \psi_{\sigma^2}] = \int_{\mathcal{D}} y \bar{\xi} d^2x. \quad (42)$$

The Casimirs, in turn, are given by

$$\mathcal{C}_{a,F}[\bar{\xi}, \psi_\sigma, \psi_{\sigma^2}] := \int_{\mathcal{D}} a \bar{\xi} + F(\psi_\sigma, \psi_{\sigma^2}) d^2x \quad (43)$$

for any constant a and arbitrary function F . In [BV21c] we presented the proof for the $IL^{(0,1)}$ PE's Casimirs (cf. Remark 8, below). Here we present the proof for the QG case. A genuine Casimir $\mathcal{C}[\bar{\xi}, \psi_\sigma, \psi_{\sigma^2}]$ must satisfy:

$$\begin{pmatrix} \{\bar{\xi}, \cdot\}_{xy} & \{\psi_\sigma, \cdot\}_{xy} & \{\psi_{\sigma^2}, \cdot\}_{xy} \\ \{\psi_\sigma, \cdot\}_{xy} & 0 & 0 \\ \{\psi_{\sigma^2}, \cdot\}_{xy} & 0 & 0 \end{pmatrix} \begin{pmatrix} \frac{\delta \mathcal{C}}{\delta \bar{\xi}} \\ \frac{\delta \mathcal{C}}{\delta \psi_\sigma} \\ \frac{\delta \mathcal{C}}{\delta \psi_{\sigma^2}} \end{pmatrix} = \begin{pmatrix} 0 \\ 0 \\ 0 \end{pmatrix}. \quad (44)$$

From the last two rows, it is clear that $\frac{\delta}{\delta \bar{\xi}}\mathcal{C}$ must be a constant. This makes the first term in the first row to vanish. The last two terms vanish by adding the integral of an arbitrary function of $(\psi_\sigma, \psi_{\sigma^2})$, showing that (43) indeed is a valid Casimir. In fact, there exists no Casimir more general than this.

Remark 8. An important difference with the $IL^{(0,1)}$ PE, omitted in [BV21c], is that for $\mathcal{C}_{a,F}$ to commute with any functional in (32), the boundaries need not be isopycnic. The $IL^{(0,1)}$ PE Casimirs are given by $\mathcal{C}_{a,F}[\bar{\mathbf{u}}, h, \bar{\vartheta}, \vartheta_\sigma] := \int_{\mathcal{D}} a \bar{q} h + F(\bar{\vartheta}, \vartheta_\sigma) d^2x$ for $a = \text{const}$ and every F where \bar{q} is the potential vorticity, which reduce to (43) in the QG limit.

The conservation laws above can all be verified directly. Indeed, one can easily compute

$$\dot{\mathcal{E}} = \bar{\psi}|_{\partial\mathcal{D}_-} \dot{\gamma}_- + \bar{\psi}|_{\partial\mathcal{D}_+} \dot{\gamma}_+, \quad (45)$$

which only vanishes when the velocity circulations along the walls of the zonal channel domain are constant, justifying the need of condition (23). As for the zonal momentum, one has that

$$\dot{\mathcal{M}} = \int_{\mathcal{D}} (\nabla^2 \bar{\psi} - R_S^{-2} \bar{\psi} + \beta y) \partial_x \bar{\psi} d^2x = 0, \quad (46)$$

where the first equality follows upon cancellation of boundary terms by virtue of (5) and the second one by using (5b), in particular. In turn, verifying the constancy of $\mathcal{C}_{a,F}$ directly is a straightforward application of boundary conditions (5).

Finally, the IL^0QG has the same motion integrals as above with R_S replaced by R in the (30) and, in particular, with (43) replaced by

$$\mathcal{C}_{F,G}[\bar{\xi}, \psi_\sigma, \psi_{\sigma^2}] := \int_{\mathcal{D}} \bar{\xi} F(\psi_\sigma) + G(\psi_\sigma) d^2x \quad (47)$$

for arbitrary F, G , which commutes with any functional with the appropriate Lie–Poisson bracket. This Casimir is well known [MH84, Ben84]. To verify conservation of energy and zonal momentum directly one simply proceeds as above. Verifying conservation of (47) directly involves some work, similar to that one involved in verifying constancy of (48), below.

2.7.2 Non-Casimir, non-explicit-symmetry-related conservation laws

Lemma 1. *The dynamics of the $IL^{(0,1)}QG$ preserve the following infinite family of functionals*

$$\mathcal{I}_F[\bar{\xi}, \psi_\sigma, \psi_{\sigma^2}] := \int_{\mathcal{D}} \bar{\xi} F(\psi_\sigma - \frac{2}{3}\psi_{\sigma^2}) d^2x \quad (48)$$

where F is arbitrary.

Proof. Since $\nabla \cdot \nabla^\perp \bar{\psi} = 0$, from (4b)–(4c) one has

$$\partial_t G(\psi_\sigma, \psi_{\sigma^2}) + \nabla \cdot G(\psi_\sigma, \psi_{\sigma^2}) \nabla^\perp \bar{\psi} = 0 \quad (49)$$

for every G . Integrating over \mathcal{D} ,

$$\int_{\mathcal{D}} G(\psi_\sigma, \psi_{\sigma^2}) d^2x = \text{const} \quad (50)$$

because the flow normal to the channel walls vanishes and there is periodicity in the along-channel direction. Now define $\phi := \psi_\sigma - \frac{2}{3}\psi_{\sigma^2}$. Multiplying (4a) by $F(\phi)$ for any F and using (49) with $G(\psi_\sigma, \psi_{\sigma^2})$ replaced by $F(\phi)$,

$$\partial_t (\bar{\xi} F(\phi)) + \nabla \cdot \bar{\xi} F(\phi) \nabla^\perp \bar{\psi} = R_S^{-2} F(\phi) \nabla \cdot \phi \nabla^\perp \bar{\psi}. \quad (51)$$

Multiplying (50) by R_S^{-2} with $G(\psi_\sigma, \psi_{\sigma^2})$ replaced by $\int F(\phi) d\phi$, and subtracting the result from (51), upon integrating over \mathcal{D} ,

$$\int_{\mathcal{D}} \bar{\xi} F(\phi) + R_S^{-2} \int F(\phi) d\phi d^2x = \text{const}. \quad (52)$$

More generally, with (50) in mind,

$$\int_{\mathcal{D}} \bar{\xi} F(\phi) + R_S^{-2} \int F(\phi) d\phi + G(\psi_\sigma, \psi_{\sigma^2}) d^2x = \text{const}, \quad (53)$$

from which conservation of (48) follows by $G(\psi_\sigma, \psi_{\sigma^2}) = -R_S^{-2} \int F(\phi) d\phi$ for arbitrary F . \square

An important observation is that the integrals of motion (48) do *not* constitute Casimirs. Indeed,

$$\begin{pmatrix} \{\bar{\xi}, \cdot\}_{xy} & \{\psi_\sigma, \cdot\}_{xy} & \{\psi_{\sigma^2}, \cdot\}_{xy} \\ \{\psi_\sigma, \cdot\}_{xy} & 0 & 0 \\ \{\psi_{\sigma^2}, \cdot\}_{xy} & 0 & 0 \end{pmatrix} \begin{pmatrix} \frac{\delta \mathcal{I}}{\delta \bar{\xi}} = F \\ \frac{\delta \mathcal{I}}{\delta \psi_\sigma} = \bar{\xi} F' \\ \frac{\delta \mathcal{I}}{\delta \psi_{\sigma^2}} = -\frac{2}{3} \bar{\xi} F' \end{pmatrix} = \begin{pmatrix} 0 \\ -\frac{2}{3} \{\psi_\sigma, \psi_{\sigma^2}\}_{xy} F' \\ \{\psi_{\sigma^2}, \psi_\sigma\}_{xy} F' \end{pmatrix}, \quad (54)$$

where the last two rows in general do not vanish. That is, \mathcal{I}_F does not commute with every functional in (32). To the best of our knowledge, this result, namely, *the existence of conservation laws unrelated to time or space symmetry which do not constitute Casimirs*, has so never been reported.

Remark 9. The $IL^{(0,1)}$ PE conserves $\int_{\mathcal{D}} \bar{q} h F(\bar{\vartheta} - \frac{1}{3} \vartheta_\sigma) d^2x$ for every F (where \bar{q} is the potential vorticity). These reduce to (48). The difference between the $\frac{1}{3}$ and $\frac{2}{3}$ factors is clarified upon noting that, with $O(\text{Ro}^2)$ error, $\bar{\vartheta} - g_r - \frac{1}{3}(\vartheta_\sigma - \frac{1}{2} N_r^2 H_r) = \frac{2g_r}{f_0 R^2}(\psi_\sigma - \frac{2}{3} \psi_{\sigma^2})$. The conservation laws above are not Casimirs either. We speculate that their existence should be attributed to invariance of the Eulerian variables under relabeling of fluid particles. The Noether theorem that should lead to this conclusion differs from the one discussed above as it should arise from the Euler–Poincaré variational principle with variations not restricted to vanish at the endpoints of the action integral, as considered by [CH12] for other systems.

3 Linear waves and free energy

Let $\varphi' := (\bar{\xi}', \psi'_\sigma, \psi'_{\sigma^2})$ be an infinitesimal-amplitude perturbation on

$$\Phi_r := (-R_S^{-2}(a_1 - a_2 + \frac{2}{3}a_3) + \beta y, a_2, a_3), \quad (55)$$

where a_1, a_2, a_3 are arbitrary constants. The latter represents a three-parameter family of *reference states*, i.e., stationary or equilibrium solutions of the $IL^{(0,1)}$ QG system (4), subjected to (5) and (23), with *no* currents. The energy of such states, $\mathcal{E}[\Phi_r] = \frac{1}{2} R_S^{-2} a_1^2 W L$. This identically vanishes for the particular class of reference states with $a_1 = 0$. Such a two-parameter family of reference states has the lowest possible energy and can thus be

identified with the *vacuum state* [e.g., ME86] of the IL^(0,1)QG. The components of the perturbation field φ' evolve according to

$$\partial_t \bar{\xi}' + \beta \partial_x \bar{\psi}' = 0, \quad \partial_t \psi'_\sigma = 0, \quad \partial_t \psi'_{\sigma^2} = 0, \quad (56)$$

controlling the IL^(0,1)QG linearized dynamics around (55). Assuming an (x, y, t) -dependence of the form of a normal mode, viz., $\exp i(kx - \omega t) \sin ly$, satisfying the boundary conditions (5), it follows that $\psi'_\sigma = 0 = \psi'_{\sigma^2}$ while $\bar{\xi}' = \nabla^2 \bar{\psi}' - R_S^{-2} \bar{\psi}' \neq 0$ provided that

$$\omega = -\frac{k\beta}{k^2 + l^2 + R_S^{-2}}, \quad (57)$$

where $lW = n\pi$, $n = 1, 2, \dots$. That is, the linear waves supported by the IL^(0,1)QG are the well-known (planetary) Rossby waves [e.g. Ped82], which do not disturb the reference buoyancy field $g_r + (1 + \frac{2z}{H_r})^{\frac{1}{2}} N_r^2 H_r$. They correspond to the Rossby waves of the HLQG in the weak-stratification limit $S \downarrow 0$. For finite S , the (westward) phase speed is in general slower. For instance, in the infinitely wide zonal channel case, the fastest phase speed, realized in the short-wave limit $(k, l) \downarrow (0, 0)$, is $\beta(1 - \frac{1}{3}S)R^2$, which can be up to one-third slower than that in the HLQG, given by βR^2 . In addition to the Rossby waves, the IL^(0,1)QG supports an $\omega = 0$, i.e., neutral, mode with $\bar{\xi}' = R_1^{-2}(\psi'_\sigma - \frac{2}{3}\psi'_{\sigma^2})$ with $\psi'_\sigma, \psi'_{\sigma^2} \neq 0$. This neutral mode is characterized by potential vorticity changes exclusively due to buoyancy changes which do not alter the fluid velocity ($\bar{\psi}' = 0$).

One test of the well-posedness of the the IL^(0,1)QG is given by the computation of the *free energy* [Rip95]. Denoted by $\mathcal{E}_{\text{free}}$, this is defined as an integral of motion quadratic to the lowest-order in the deviation from a reference state. When $\mathcal{E}_{\text{free}}$ is positive definite, there cannot be a spurious growth of the amplitude of linear waves riding on the reference state as they must preserve $\mathcal{E}_{\text{free}}$. A class of reference states (55) with a free energy with the desired property is defined by $\frac{a_1}{a_2} < 0$ and $\frac{a_1}{a_3} > 0$. Indeed, for such a class of reference states,

$$\mathcal{E}_{\text{free}}[\bar{\xi}', \psi'_\sigma, \psi'_{\sigma^2}] = \mathcal{E}[\bar{\psi}'] + R_S^{-2} \int_{\mathcal{D}} \frac{2}{3} \frac{a_1}{a_3} \psi'^2_{\sigma^2} - \frac{a_1}{a_2} \psi'^2_{\sigma} d^2x, \quad (58)$$

which is manifestly positive definite under the stated conditions. This follows by adding to the energy (30) a Casimir (43) with $a = a_1$ and $F(\psi_\sigma, \psi_{\sigma^2}) = R_S^{-2}(\frac{a_1}{3a_3}\psi_{\sigma^2}^2 - \frac{a_1}{2a_2}\psi_\sigma^2)$. An important observation is that (58) is not restricted to infinitesimally small normal-mode perturbations. In fact, (58) is an exact integral of motion for the fully nonlinear dynamics about (55). Thus positive definiteness of (58) prevents the spurious growth of perturbations to (55) irrespective of their initial amplitude and structure.

It is fair to wonder about the dynamical significance of the constants a_1, a_2, a_3 that define the family of reference states (55) and the relationship among them for $\mathcal{E}_{\text{free}}$ to be positive definite. Consider the situation in which these constants are all set to zero, in which case (55) reduces $\Phi_r = (\beta y, 0, 0)$, a member of the vacuum state family. The linear waves riding on this reference state are the same as those discussed above. However, in

this case, the free energy can be shown to be equal to $\mathcal{E}[\bar{\psi}']$, which is positive semidefinite. Indeed, by the invertibility relationship (4d), it follows that there can be perturbations $(\bar{\xi}', \psi'_{\sigma}, \psi'_{\sigma^2})$ that do not change the free energy. Spontaneous growth of the amplitude of such perturbations cannot be constrained by free-energy conservation. An example is the neutral mode discussed above, for which the free energy identically vanishes. The same considerations apply to the complete family of vacuum states (defined by $a_1 = 0$). An important observation is that there exist Lyapunov stable states that will arrest the aforementioned spontaneous growth, should it happened, as discussed in Section 5, below.

Remark 10. *A result similar to that for perturbations on the vacuum state family in the $IL^{(0,1)}$ QG holds for perturbations on the vacuum state in the $IL^{(0,1)}$ PE parent model. In that model, there is a unique reference state, which is the vacuum state, and perturbations on it have a positive-semidefinite free energy associated with [cf. Rip95].*

4 Stability of baroclinic zonal flow

Consider $\varphi := (\bar{\xi}, \psi_{\sigma}, \psi_{\sigma^2})$, evolving according to (4) subjected to (5) and (23). We call $\Phi := (\bar{\Xi}, \Psi_{\sigma}, \Psi_{\sigma^2})$ a *basic state* if it is an equilibrium of (4), subjected to (5) and (23). A particular case of basic state is the reference state discussed in Section 3, for which the fluid is motionless. We are interested in the stability of a basic state in the following three senses, sorted in increasing level of strength [HMRW85, Rip00].

- The first sense is *spectral stability*, in which case a perturbation $\delta\varphi(\mathbf{x}, t)$ on $\Phi(\mathbf{x})$ is assumed to be a normal mode with an infinitesimally small amplitude, viz., $\delta\varphi = \varepsilon \text{Re}\{\varphi' \exp ik(x - ct)\} \sin ly + O(\varepsilon^2)$ where $\varepsilon \downarrow 0$, satisfying (5) and (23). (Note the slight change of interpretation of the prime notation with respect to that used in Section 3.) Clearly, the amplitude of a normal mode cannot remain infinitesimally small unless $\text{Im}(c) = 0$. In such a case, the basic state is said to be spectrally stable.
- The second sense is *formal stability*. In this case $\delta\varphi$, while assumed small, can have an arbitrary structure. If there exists an integral of motion $\mathcal{H}[\varphi]$ such that $\delta\mathcal{H}[\delta\varphi; \Phi] = 0$ and $\delta^2\mathcal{H}[\delta\varphi; \Phi] > 0$, then the growth of $\delta\varphi$ will be constrained. The constraint is imposed by the quadratic nature of $\delta^2\mathcal{H}$, which is preserved by the linearized dynamics about Φ . In these circumstances one says that Φ is formally stable. Note that $\mathcal{E}_{\text{free}}$ is a special case of $\delta^2\mathcal{H}$ wherein Φ is motionless (cf. Section 3).
- The third sense is *Lyapunov stability*. This relies on the possibility of proving that the total variation $\Delta\mathcal{H}[\delta\varphi; \Phi]$ is convex for finite-size $\delta\varphi$ of arbitrary structure. This means showing that $c_1\|\delta\varphi\|^2 \leq \Delta\mathcal{H} \leq c_2\|\delta\varphi\|^2$ for $c_1, c_2 = \text{const}$ such that $0 < c_1 \leq c_2 < \infty$, where $\|\cdot\|$ is typically chosen to be an L^2 norm. Assuming that the latter holds true, since $\Delta\mathcal{H}$ is preserved under the fully nonlinear dynamics, the second

inequality can be evaluated at time $t = 0$ to get $\|\delta\varphi\|_{t>0} \leq \sqrt{\frac{c_2}{c_1}} \|\delta\varphi\|_{t=0}$. This implies Lyapunov stability for Φ . More precisely, for every $\varrho > 0$ there exists $\varepsilon > 0$, e.g., $\varepsilon = \sqrt{\frac{c_1}{c_2}} \varrho$, such that $\|\delta\varphi\|_{t=0} < \varepsilon$ implies $\|\delta\varphi\|_{t>0} < \varrho$.

Let

$$\alpha := \frac{\bar{U}}{U_\sigma}, \quad \mu := \frac{U_{\sigma^2}}{U_\sigma}, \quad b := \frac{\beta}{U_\sigma R^2}, \quad (59a)$$

where \bar{U} , U_σ , and U_{σ^2} are constants, with the latter two required to satisfy

$$2U_\sigma - U_{\sigma^2} \geq \frac{(S-1)f_0 R^2}{2W}, \quad U_{\sigma^2} < \frac{Sf_0 R^2}{4W}, \quad (59b)$$

by static stability; cf. (2). Our main interest is the four-parameter family of basic states defined by

$$\bar{\Psi} = -\bar{U}y, \quad \Psi_\sigma = -U_\sigma y, \quad \Psi_{\sigma^2} = -U_{\sigma^2}y, \quad (59c)$$

implying

$$\bar{\Xi} = -R_S^{-2} \bar{\Psi} + R_S^{-2} (\Psi_\sigma - \frac{2}{3} \Psi_{\sigma^2}) + \beta y = R_S^{-2} \nu \Psi_\sigma = R_S^{-2} \mu^{-1} \nu \Psi_{\sigma^2}, \quad (59d)$$

where

$$\nu(S) := 1 + \alpha + s(S)b - \frac{2}{3}\mu, \quad s(S) := R_S^2 R^{-2} = 1 - \frac{1}{3}S, \quad (59e)$$

which we introduce to simplify algebraic expressions below. By the thermal-wind balance, (59) implicitly corresponds, for parameters fixed, to a meridionally uniform zonal current with quadratic vertical shear, i.e., a baroclinic flow with vertical curvature on the β -plane. Nondimensional parameters α and μ thus measure the vertical linear shear and curvature of the jet, respectively. But, by virtue of (9)–(11), one also has that

$$\alpha = 1 + \frac{2sg_r}{H_r} \frac{H'(y)}{\bar{\Theta}'(y)} - \frac{H_r}{6} \frac{(N^2)'(y)}{\bar{\Theta}'(y)}, \quad \mu = \frac{H_r}{4} \frac{(N^2)'(y)}{\bar{\Theta}'(y)}, \quad (60)$$

where H is the layer thickness in the basic state, $\bar{\Theta}$ is the basic vertically averaged buoyancy, and $N^2 = 2\frac{\Theta_r}{H_r}$ is the basic state buoyancy frequency squared. This enables further physical insight into the (spectral) stability problem. Finally, nondimensional parameter b measures the strength of the β effect, which can be identified with a Charney number.

4.1 Spectral stability

Let

$$\lambda := \frac{c - \bar{U}}{U_\sigma}, \quad \kappa := R\sqrt{k^2 + l^2}, \quad (61)$$

representing normalized Doppler shifted phase speed and wavenumber $\mathbf{k} = (k, l)$ (with k pointing eastward and l northward) magnitude, respectively. The following eigenvalue problem follows upon proposing a normal-mode perturbation on (59):

$$\begin{pmatrix} (s\kappa^2 + 1)\lambda + \alpha + sb & -(\lambda + \alpha) & \frac{2}{3}(\lambda + \alpha) \\ -1 & -\lambda & 0 \\ -\mu & 0 & -\lambda \end{pmatrix} \begin{pmatrix} \bar{\psi}' \\ \psi'_\sigma \\ \psi'_{\sigma^2} \end{pmatrix} = 0. \quad (62)$$

Nontrivial solutions exist provided that the determinant of the matrix of the eigenproblem vanishes. This leads to the dispersion relation

$$\lambda = \frac{-\nu \pm \sqrt{\nu^2 - 4\alpha(1 - \frac{2}{3}\mu)(s\kappa^2 + 1)}}{2(s\kappa^2 + 1)}. \quad (63)$$

Spectral stability is realized when the perturbation phase speed c , or equivalently λ , is real. A sufficient condition for this is

$$\alpha(1 - \frac{2}{3}\mu) < 0. \quad (64)$$

The shaded quadrants in Fig. 2 are subsets of the region in the (α, μ) -space defined by (64), namely,

$$\{\alpha < 0\} \cap \{\mu < \frac{3}{2}\} \cup \{\alpha > 0\} \cap \{\mu > \frac{3}{2}\}, \quad (65)$$

where there is spectral stability of basic state (59) for every wavenumber. *This holds independent of the values taken by the Charney number (b) and stratification parameter (S).* By virtue of (60), one concludes that the basic states in the upper-right (resp., lower-left) clear quadrant have $H'(y)$ and $\bar{\Theta}'(y)$ with like (resp., opposing) signs and $\frac{\bar{\Theta}'(y)}{(N^2)'(y)}$ smaller (resp., larger) than $\frac{1}{6}H_r$. The curves labeled by κ bound the (sub)regions of the (α, μ) -plane where there is spectral instability, i.e., (64) is violated, for selected b and S values. Note the asymmetry, with less basic states being spectrally unstable toward smaller wavenumbers in the region $\{\alpha < 0\} \cap \{\mu > \frac{3}{2}\}$ than in the region $\{\alpha > 0\} \cap \{\mu < \frac{3}{2}\}$. This behavior reverses with positive values of b .

More specifically, in the limit $\kappa \downarrow 0$, (67) equals

$$\lambda = -\frac{1}{2}\nu \pm \frac{1}{2}\sqrt{\nu^2 - 4\alpha(1 - \frac{2}{3}\mu)}, \quad (66)$$

which is complex where $\alpha(1 - \frac{2}{3}\mu) > \frac{1}{4}\nu^2 = \frac{1}{4}(1 + \alpha + sb - \frac{2}{3}\mu)^2$ (and real otherwise, making explicit that (64) is sufficient, yet not necessary, for spectral stability). At criticality, $\mu = \frac{3}{2}(1 - \alpha + sb) \pm \frac{3}{2}\sqrt{(1 - \alpha + sb) - (1 + \alpha + sb)^2 + 4\alpha}$. This represents a parabola with tangencies on the curve $C_+ := \{\alpha = 0, \mu > \frac{3}{2}\} \cup \{\alpha > 0, \mu = \frac{3}{2}\}$, when $b < 0$, and the curve $C_- := \{\alpha = 0, \mu < \frac{3}{2}\} \cup \{\alpha < 0, \mu = \frac{3}{2}\}$, when $b > 0$, making more explicit the asymmetry noted above. For completeness, we note that in the limit $\kappa \uparrow \infty$ there is

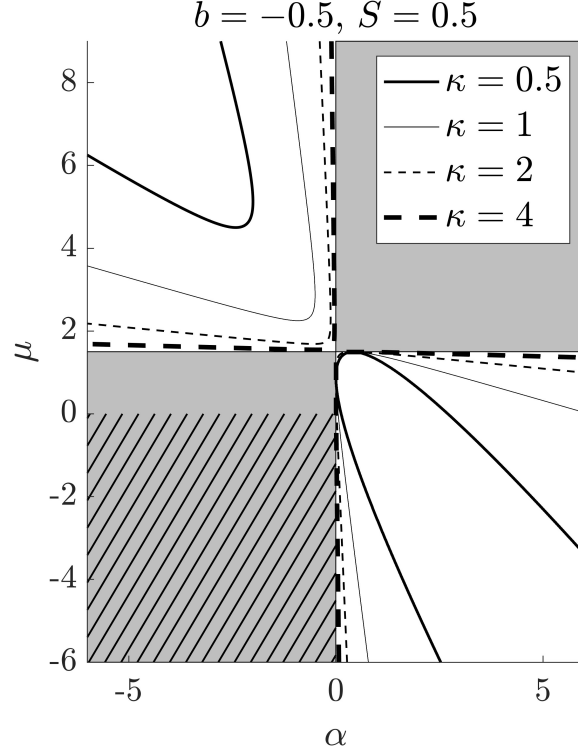


Figure 2: Stability of the basic state family (59), representing baroclinic zonal jets, in the $\alpha := \bar{U}/U_\sigma$ vs $\mu := U_{\sigma 2}/U_\sigma$ space, respectively measuring the vertical linear shear and curvature of a jet in the family. In the shaded regions, corresponding to a subset of $\alpha(1 - \frac{2}{3}\mu) \leq 0$, the phase speed of an infinitesimally-small normal-mode perturbation is real for all wavenumbers. The hatched region, a subset of $\{\mu < 0\} \cap \{\alpha < 0\}$, there is stability for finite-size perturbations of arbitrary structure. Moreover, in that region the distance, in an L^2 sense, of a perturbation to the basic state is at all times bounded by a multiple of its initial distance. This means that in the hatched region there is Lyapunov stability. Spectral stability is possible in the white regions, where the curves labeled by the normalized wavenumber magnitude $\kappa := R\sqrt{k^2 + l^2}$ bound the (α, μ) -subregions where there is spectral instability for the normalized β and stratification parameters, $b := \beta/U_\sigma R^2$ and $S := N_r^2 H_r/2g_r$, respectively, as indicated.

spectral stability everywhere in the (α, μ) -space where (64) is violated, in such a case for any b and S . Indeed,

$$\lambda \sim \pm i \sqrt{\frac{\alpha(1 - \frac{2}{3}\mu)}{1 - \frac{1}{3}S}} \kappa^{-1} \quad (67)$$

asymptotically as $\kappa \uparrow \infty$. The curves $\kappa \uparrow \infty$ in the (α, μ) -plane are given by C_\pm . Their

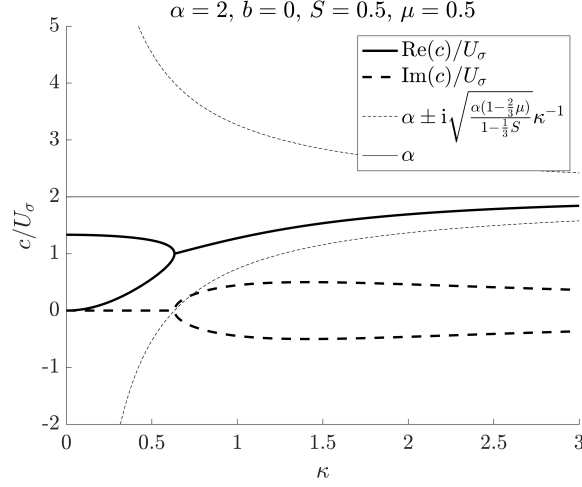


Figure 3: As a function of normalized wavenumber, normalized phase speed for a normal-mode perturbation on the baroclinic zonal jet defined by (59) with parameters as indicated. Asymptotic dispersion relation curves as $\kappa \uparrow \infty$ and the corresponding limiting value are included.

union $\{\alpha = 0, \mu = \frac{3}{2}\}$ corresponds to the set of basic states lying at the boundary of spectral stability. Thus, unlike all other curves in the spectrally unstable regions of the (α, μ) -plane, the curves C_{\pm} do not bound spectrally unstable states.

In Fig. 3 we depict dispersion relation (63) as a function of the wavenumber, more precisely $\frac{c}{U_{\sigma}}$ vs κ , for selected values of the various basic state parameters. The onset of instability happens at the wavenumber where the two branches of the dispersion relation merge. Included in the plot for reference is the asymptotic expression for $\frac{c}{U_{\sigma}}$ as $\kappa \uparrow \infty$, as it follows from (67). Also indicated is $\lim_{\kappa \uparrow \infty} \frac{c}{U_{\sigma}} = \alpha$, that is, a real number, irrespective of the parameters that define the basic state.

In the limit of weak stratification, i.e., $S \downarrow 0$, the length scales R and $L := \frac{N_r H_r}{|f_0|}$ are well separated. The latter is proportional to the gravest baroclinic (internal) Rossby radius of deformation in a model with arbitrary stratification. Since we are assuming a reduced-gravity setting, R and L can be approximately identified with the first and second internal deformation radii, respectively, of the arbitrarily stratified model extending throughout the entire water column. The noted scale separation allows one to distinguish long perturbations, with wavenumbers $\kappa = O(1)$ as $S \downarrow 0$, from short perturbations, with wavenumbers $L|\mathbf{k}| = \sqrt{2S}\kappa = O(1)$ as $S \downarrow 0$. We find that (63) reduces to

$$\lambda = \frac{-\nu(0) \pm \sqrt{\nu(0)^2 - 4\alpha \left(1 - \frac{2}{3}\mu\right) (\kappa^2 + 1)}}{2(\kappa^2 + 1)}, \quad (68)$$

for long perturbations, and $\lambda = 0$, for short perturbations. The limit $\kappa \uparrow \infty$ of (68) gives

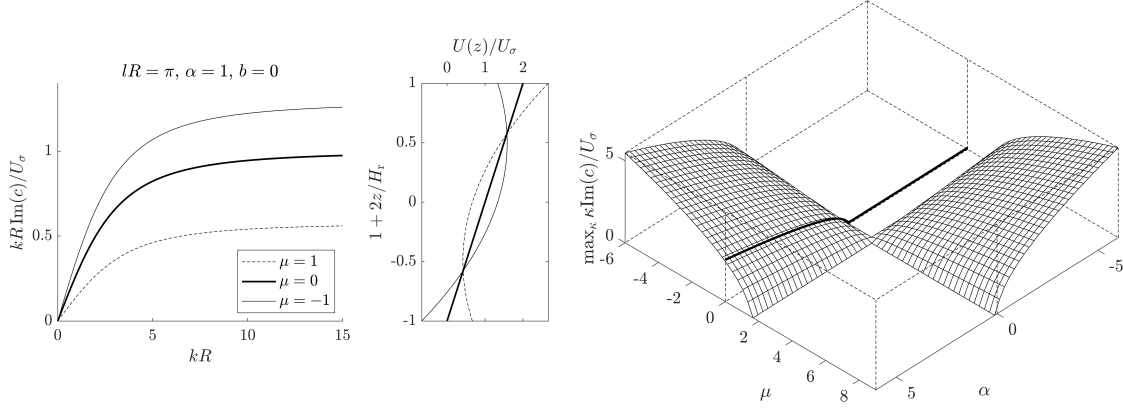


Figure 4: (right) Growth rate as a function of zonal wavenumber in the limit of weak stratification ($S \downarrow 0$) with basic state parameters α and b as indicated for three values of μ . The IL⁰QG result corresponds to the $\mu = 0$ curve as the velocity in that model can only include linear shear (implicitly, by the thermal-wind balance). (middle) Zonal velocity (implicit) vertical profiles leading to the growth rates in the left panel. (left) Upper bound on the growth rate in (α, μ) -space for weak stratification. The thick line is the corresponding result for the IL⁰Q.

$\lambda = 0$, i.e., $c = \bar{U}$. As expected, it coincides with the short-perturbation phase speed. This is real for all wavenumbers, which can be anticipated to be consequential for direct, fully nonlinear simulations. It seems reasonable to think that wave activity in such simulations will fall off at sufficiently large wavenumbers (short wavelengths), which, according to the spectral (i.e., linear) analysis, are not growing.

As for the growth rate of the perturbation, given by $\varpi := k \text{Im}(c)$ for the smallest meridional wavenumber, viz., $l = \frac{\pi}{W}$, this saturates with zonal wavenumber, both when the stratification is finite and for long perturbations in the weak-stratification limit. The left panel of Fig. 4 shows $\varpi(k)$ when $W = R$ for selected values of basic state parameters outside the spectrally stable set (65) in the limit of weak stratification and with vanishing Charney number. Note that ϖ is larger (resp., smaller) when the basic state zonal velocity vertical profile (Fig. 4, middle panel) curves eastward (resp., westward) than when it does not curve, as in the IL⁰QG. An upper-bound measure of the saturating value of ϖ is given, when S is finite, by

$$\max_\kappa \frac{\kappa \text{Im}(c)}{U_\sigma} = \sqrt{\frac{\alpha(1 - \frac{2}{3}\mu)}{1 - \frac{1}{3}S}}, \quad (69)$$

where parameters (α, μ) belong in the spectrally unstable region, i.e., the complement of set (65). The long-perturbation limit of (69) is $\sqrt{\alpha(1 - \frac{2}{3}\mu)}$, which we plot in right panel of Fig. 4. An important final observation, with consequences for direct simulations, is that the growth rate for short perturbations vanishes for all wavenumbers, reinforcing the

comments above that development of wave activity should be stopped in the IL^(0,1)QG at sufficiently short wavelengths.

4.2 Formal stability

We now turn to investigate the formal stability of basic states (59), for which we have at our disposal several conservation laws, namely, energy (\mathcal{E}), Casimirs ($\mathcal{C}_{a,F}$), zonal momentum (\mathcal{M}), and the non-Casimir, non-explicit-symmetry-related conservation laws (\mathcal{I}_F) (cf. Section 2.7) to construct an appropriate general integral of motion \mathcal{H} such that $\delta\mathcal{H} = 0$ at a basic state. The use of energy and Casimirs to construct \mathcal{H} may be traced from the work of [Arn14] back over a decade to those of [Fj50, KO58]. The use of momentum in systems with x -translational symmetry was pioneered by Ripa [Rip83]. Here we explore the additional use of the new conservation law \mathcal{I}_F . We these comments in mind, we will, following tradition, refer to the use of all available integrals of motion to derive a-priori stability statements as *Arnold's method*.

Remark 11. *A few remarks are in order.*

1. *The equilibria Φ of a Hamiltonian system $\partial_t\varphi = \{\varphi, \mathcal{E}\}$ are no longer unrestricted conditional extrema of the Hamiltonian (\mathcal{E}); by contrast, $\partial_t\Phi = \{\Phi, \mathcal{E}[\Phi]\}[\Phi] = 0$ implies that $\frac{\delta}{\delta\varphi}(\mathcal{E} + \mathcal{C})[\Phi] = 0$ for some Casimir \mathcal{C} . Level sets of constants of the motion define certain “leaves” on the Poisson manifold, $(P, \{, \})$. If these constants are the Casimirs of $\{, \}$, they form the “symplectic leaves” of P [e.g., HMRW85, Mor98]. Thus equilibria (basic states) are critical “points” of \mathcal{E} restricted to such leaves.*
2. *When \mathcal{H} is chosen to be a linear combination $\mathcal{E} + \mathcal{C} - U\mathcal{M}$ where $U = \text{const}$ and for some \mathcal{C} such that $\delta\mathcal{H} = 0$ at Φ , it turns out that $\delta^2\mathcal{H}$ is a Hamiltonian for the linearized dynamics about Φ as seen from a reference frame steadily translating in the x -direction with speed U . Namely, to the lowest order in $\delta\varphi$, it follows that $(\partial_t + U\partial_x)\delta\varphi = \{\delta\varphi, \delta^2\mathcal{H}\}[\Phi]$ where the bracket here is that defined in (32) but with a constant argument. This is a genuine Lie–Poisson bracket in that all required properties are satisfied, most importantly the Jacobi identity, which is readily verified [cf., ME86, for a discussion]*
3. *With \mathcal{H} as constructed, the integral $\delta^2\mathcal{H}$, or more generally $\Delta\mathcal{H}$, is referred to as pseudoenergy–momentum, following notation introduced in [Rip83]. In the case with no zonal symmetry, the pseudoenergy is referred to as a “free energy” in [Mor98] to mean that it is the energy accessible to the system upon perturbation away from equilibrium given the Casimir. It should not be confused with the free energy defined in Section 3.*

We begin by considering

$$\mathcal{H}_{\bar{U}} := \mathcal{E} - \bar{U}\mathcal{M} + \mathcal{C}_{0,F} \quad (70)$$

with

$$F(\psi_\sigma, \psi_{\sigma^2}) = -\frac{1}{2}\alpha R_S^{-2} (\psi_\sigma^2 - \frac{2}{3}\mu^{-1}\psi_{\sigma^2}^2). \quad (71)$$

The first variation of (70) identically vanishes at the basic state (59). Its second variation

$$\delta^2 \mathcal{H}_{\bar{U}} = \mathcal{E}[\delta\bar{\psi}] - \frac{1}{2}R_S^{-2}\alpha \int \delta\psi_\sigma^2 - \frac{2}{3}\mu^{-1}\delta\psi_{\sigma^2}^2 d^2x, \quad (72)$$

which is positive definite provided that

$$\alpha < 0, \quad \mu < 0. \quad (73)$$

This corresponds to the hatched region of the (α, μ) -plane of Fig. 2. That is, only a subset of the spectrally stable states are possible to be proved formally stable. But such a subset however is stable with respect to perturbations not only of arbitrary structure. Rather, they are stable with respect to finite-amplitude perturbations since

$$\delta^2 \mathcal{H}_{\bar{U}} = \Delta \mathcal{H}_{\bar{U}}. \quad (74)$$

That is, the pseudoenergy–momentum is a quadratic integral of motion. This is a Hamiltonian for the exact dynamics of the $\text{IL}^{(0,1)}$ as seen by an observer zonally moving with speed \bar{U} (extending Remark 11.2, above). We will return to discussing the consequences of (74) in Section 4.3, below.

Let us consider now the use of the new conservation laws \mathcal{I}_F , defined in (48), in Arnold's method. It turns out that the general integral of motion

$$\mathcal{H}_{\frac{2}{3}\alpha U_\sigma} := \mathcal{E} - \frac{2}{3}\alpha U_\sigma \mathcal{M} + \mathcal{C}_{0,F} + \mathcal{I}_G \quad (75)$$

for

$$F(\psi_\sigma, \psi_{\sigma^2}) = \frac{1}{2}R_S^{-2}\alpha(\nu+1) \left(\frac{2}{3}\nu^{-1}\psi_{\sigma^2}^2 - \psi_\sigma^2 \right), \quad (76)$$

$$G(\psi_\sigma - \frac{2}{3}\psi_{\sigma^2}) = \alpha \left(\psi_\sigma - \frac{2}{3}\psi_{\sigma^2} \right), \quad (77)$$

has a vanishing first variation at the basic state (59). Its second variation,

$$\begin{aligned} \delta^2 \mathcal{H}_{\frac{2}{3}\alpha U_\sigma} &= \mathcal{E}[\delta\bar{\psi}] + \alpha \int \left(\delta\bar{\xi} + \frac{1}{2}\delta\psi_\sigma \right)^2 - \left(\delta\bar{\xi} + \frac{1}{3}\delta\psi_{\sigma^2} \right)^2 \\ &\quad - \frac{1}{2} \left(R_S^{-2}(\nu+1) + \frac{1}{2} \right) \delta\psi_\sigma^2 + \frac{1}{3} \left(R_S^{-2}\mu^{-1}(\nu+1) - \frac{1}{3} \right) \delta\psi_{\sigma^2}^2 d^2x. \end{aligned} \quad (78)$$

Higher-order variations of (75) vanish, so (78) is an exact, fully nonlinear conservation law. However, it is at most positive semidefinite and provided that $\alpha = 0$. Thus the new conservation laws (48) are not useful to make an a-priori assessment about the stability of the basic state (59), at least using Arnold's method.

4.3 Lyapunov stability

Lyapunov stability of the basic states defined by (73) can be established as follows. Consider the subset of stable basic states with

$$\alpha < 0, \quad 0 > \mu \geq -1. \quad (79)$$

Let η_1 and λ_1 be two positive constants such that

$$0 < \eta_1 < -\alpha \quad (80)$$

and

$$-\alpha - \eta_1 \leq \lambda_1 \leq -\alpha + \eta_1, \quad (81)$$

respectively. Recalling that (74) holds, the convexity estimate follows:

$$\frac{-\alpha - \eta_1}{\lambda_1} \|(\delta\bar{\xi}, \delta\psi_\sigma, \delta\psi_{\sigma^2})\|_2(\lambda_1)^2 \leq \Delta\mathcal{H}_{\bar{U}} \leq \frac{-\alpha + \eta_1}{\lambda_1} \|(\delta\bar{\xi}, \delta\psi_\sigma, \delta\psi_{\sigma^2})\|_2(\lambda_1)^2, \quad (82)$$

where

$$\|(\delta\bar{\xi}, \delta\psi_\sigma, \delta\psi_{\sigma^2})\|_2(\lambda_1)^2 := \mathcal{E}[\delta\bar{\psi}] + \frac{1}{2}R_S^{-2}\lambda_1 \int \delta\psi_\sigma^2 + \frac{2}{3}\delta\psi_{\sigma^2}^2 dx, \quad (83)$$

measures, in an L^2 sense, the squared distance to the subfamily of basic states (59) defined by (79) in the infinite-dimensional phase space of the IL^(0,1)QG model equation (4) with coordinates $(\bar{\xi}, \psi_\sigma, \psi_{\sigma^2})$ (cf. Remark 6). This establishes Lyapunov stability for them. Indeed, since $\Delta\mathcal{H}_{\bar{U}}$ is invariant and convex, it follows that the distance to such states at any time is bounded from above by a multiple of the initial distance.

Consider now the subfamily of basic states (59) defined by

$$\alpha < 0, \quad \mu < -1. \quad (84)$$

Letting η_2 and λ_2 be positive constants such that

$$0 < \eta_2 < \frac{\alpha}{\mu} \quad (85)$$

and

$$\frac{\alpha}{\mu} - \eta_2 \leq \lambda_2 \leq \frac{\alpha}{\mu} + \eta_2, \quad (86)$$

one finds the convexity estimate:

$$\frac{\alpha - \mu\eta_2}{\mu\lambda_2} \|(\delta\bar{\xi}, \delta\psi_\sigma, \delta\psi_{\sigma^2})\|_2(\lambda_2)^2 \leq \Delta\mathcal{H}_{\bar{U}} \leq \frac{\alpha + \mu\eta_1}{\mu\lambda_2} \|(\delta\bar{\xi}, \delta\psi_\sigma, \delta\psi_{\sigma^2})\|_2(\lambda_2)^2. \quad (87)$$

This establishes Lyapunov stability for basic states (59) with (84). Overall the above convexity estimates establish Lyapunov stability for (59) over the whole range of stable parameters (73).

5 Nonlinear saturation of unstable baroclinic zonal flow

In this section we seek to a-priori constraining the growth of perturbations to basic states (59) that have been found to be spectrally unstable, namely, those that violate (64), by making use of the above Lyapunov stability result(s) for basic states (59) satisfying (73). This can be done using *Shepherd's method*, introduced in [She88], which we outline below. Denote stable (resp., unstable) state quantities with a superscript S (resp., U). Grouping $(\bar{\xi}, \psi_\sigma, \psi_{\sigma^2})$ into φ we have

$$\|\varphi - \Phi^U\|_2(\lambda_1) \leq \sqrt{\frac{2\alpha^S}{\alpha^S + \eta_1}} \|\Phi^S - \Phi^U\|_2(\lambda_1) =: \mathcal{B}_1 \quad (88)$$

for Φ^S satisfying (79) and

$$\|\varphi - \Phi^U\|_2(\lambda_2) \leq \sqrt{\frac{2\alpha^S}{\alpha^S - \mu^S \eta_2}} \|\Phi^S - \Phi^U\|_2(\lambda_2) =: \mathcal{B}_2 \quad (89)$$

for Φ^S satisfying (84). The inequalities above follow as a result of successively:

1. applying the triangular inequality $\|\varphi - \Phi^U\|_2(\lambda_i) \leq \|\varphi - \Phi^S\|_2(\lambda_i) + \|\Phi^S - \Phi^U\|_2(\lambda_i)$, $i = 1, 2$;
2. using convexity estimate (82) for $i = 1$ and (87) for $i = 2$; and
3. assuming that $\varphi \approx \Phi^U$ initially at $t = 0$.

Set λ_1 and λ_2 to their minimum values in their corresponding admissible ranges, given by (81) and (86), respectively. Let

$$0 < r_i < 1, \quad i = 1, 2, \quad (90)$$

be constants such that

$$\eta_1 = -r_1 \alpha^S, \quad \eta_2 = r_2 \frac{\alpha^S}{\mu^S} \quad (91)$$

satisfy (80) and (85), respectively. The following tighter bounds result upon minimizing over r_i , $i = 1, 2$:

$$\mathcal{B}_1 \geq \hat{\mathcal{B}}_1 := R_S^{-1} \sqrt{\frac{1}{6} L W^3} \cdot \sqrt{(\bar{U}^S - \bar{U}^U)^2 - \frac{\bar{U}^S}{U_\sigma^S} ((U_\sigma^S - U_\sigma^U)^2 + \frac{2}{3} (U_{\sigma^2}^S - U_{\sigma^2}^U)^2)} \quad (92)$$

and

$$\mathcal{B}_2 \geq \hat{\mathcal{B}}_2 := R_S^{-1} \sqrt{\frac{1}{6} L W^3} \cdot \sqrt{(\bar{U}^S - \bar{U}^U)^2 + \frac{\bar{U}^S}{U_{\sigma^2}^S} ((U_\sigma^S - U_\sigma^U)^2 + \frac{2}{3} (U_{\sigma^2}^S - U_{\sigma^2}^U)^2)}. \quad (93)$$

In the top-left panel of Fig. 5 we plot $\hat{\mathcal{B}}_1$ in (α^U, μ^U) -space for $U_\sigma^U = 2f_0R$ as computed using $\bar{U}^S = f_0R$, $U_\sigma^S = -f_0R$, and $U_{\sigma^2}^S = \frac{1}{2}f_0R$. The top-right panel of Fig. 5 likewise shows $\hat{\mathcal{B}}_2$ as obtained with $\bar{U}^S = f_0R$, $U_\sigma^S = -f_0R$, and $U_{\sigma^2}^S = \frac{3}{2}f_0R$. Note that the bounds do not drop down to zero at the boundary of instability. They do along $\alpha^U = 0$ as $\bar{U}^S \downarrow 0$ (Fig. 5, bottom panels). However, they do not along $\mu^U = \frac{3}{2}$ because the Lyapunov-stable basic states only span a subset of complement of the spectrally stable region in the (α, μ) -space (cf. Fig. 2). Optimal bounds may be obtained by minimizing $\hat{\mathcal{B}}_1$ and $\hat{\mathcal{B}}_2$ over stable state parameters. The important point to highlight however is the existence of a-priori upper bounds which prevent perturbations to spectrally unstable basic states, namely, equilibria (59) violating (64), from undergoing an ultraviolet explosion.

Finally, as shown in [BV21b], Shepherd’s method can be used to bound the growth of perturbations on unstable states which may belong to a class different than that of those states for which Lyapunov stability can be established. As a consequence, the above conclusion can be extended to perturbations on the vacuum state, characterized by positive-semidefinite free energy (cf. Section 3), which constitutes a special form of pseudo-energy–momentum. Indeed, their nonlinear growth is constrained by the existence of Lyapunov-stable basic states as is the nonlinear growth of perturbations to unstable basic states, which have sign-indefinite pseudo-energy–momentum. Bounds on the spontaneous growth of perturbations to the vacuum state, should it is realized, are given by either (92) and (93) with $\bar{U}^U = U_\sigma^U = U_{\sigma^2}^U = 0$.

6 Discussion

The study presented here was motivated, in part, by direct numerical simulations revealing a tendency of the IL⁰QG to quickly develop visually more intense small-scale vortex rolls than the IL^(0,1)QG [BV21c]. Such small-scale circulation can be fairly referred to as submesoscale circulations as their scales fall well below R , the Rossby deformation radius in the IL⁰QG and IL^(0,1)QG models. As noted above, being R an equivalent barotropic deformation radius, it approximately corresponds to the gravest baroclinic (i.e., internal) deformation scale in the continuously stratified model defined over the entire water column. The results from the various analyses carried out above do not appear to provide reason to expect that the numerical observation of [BV21c] holds in general, as we summarize next.

- The production (or destruction) of Kelvin–Noether circulation (\mathcal{K}) along material loops was identified [HLP21] with the development of sub-deformation scale or submesoscale wave activity in the IL⁰QG. It turns out that \mathcal{K} is equally produced (or destroyed) in both the IL⁰QG and IL^(0,1)QG. The rate of change of \mathcal{K} in the former is given by (20) with the $-\frac{2}{3}\psi_{\sigma^2}$ term omitted. While by static stability one has that $-\frac{2}{3}\psi_{\sigma^2} < \frac{1}{6}f_0R^2S$, one cannot anticipate the contribution of the gradient of this term to the integral in (20). In other words, one cannot anticipate the role of stratification in the production (or destruction) of \mathcal{K} .

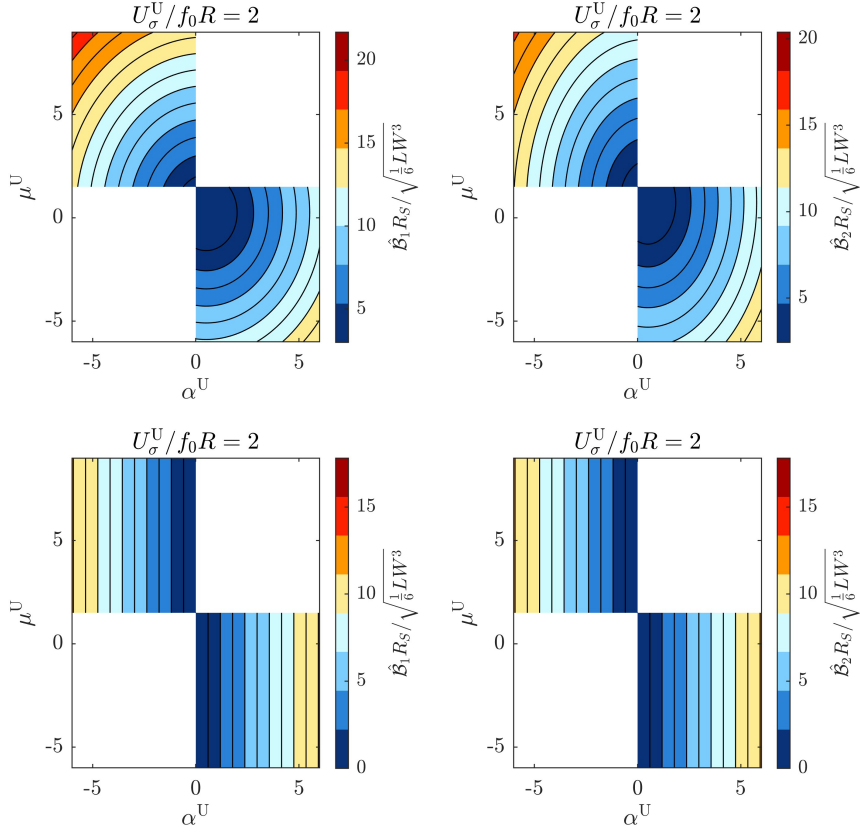


Figure 5: Normalized a-priori nonlinear upper bounds on the growth of perturbations to spectrally unstable basic states as computed using Lyapunov-stable states with $\alpha^S < 0$ and $0 > \mu^S \geq -1$ (top left) and $\alpha^S < 0$ and $\mu^S < -1$ (top right). The bottom panels show the same as in the top panels in the limit $\bar{U}^S \downarrow 0$.

- Both the IL^0QG and $\text{IL}^{(0,1)}\text{QG}$ sustain a neutral mode, referred to as a “force compensating mode” by Ripa [Rip96a], wherein potential vorticity changes due to buoyancy changes which do not alter the fluid velocity (cf. Section 3). That is, associated with this mode is vanishing free energy, which cannot constrain a possible spontaneous growth of this mode. Thus, both the IL^0QG and $\text{IL}^{(0,1)}\text{QG}$ suffer from this property, which might equally play a role in the development of submesoscale circulations in both models.
- The intensity of submesoscale motions is constrained by the existence of Lyapunov-stable states, both in the $\text{IL}^{(0,1)}\text{QG}$ (cf. Section 5) and the IL^0QG [BV21b, BV24]. However, one cannot compare the size of the space available in each model for wave activity, more precisely, the nonlinear growth of the amplitude of perturbations on

basic states (59) violating (64), the condition for spectral stability. The reason is that this is measured using different (L^2) norms.

- As for spectral stability itself, this predicts growth rates in the $\text{IL}^{(0,1)}\text{QG}$ that can be smaller than, equal to, or larger than those in the IL^0QG (cf., e.g., Fig. 4). The only, potentially important, difference is that the growth rate vanishes in the $\text{IL}^{(0,1)}\text{QG}$ for short perturbations. Distinguishing short from large perturbations in the weak stratification limit is only possible in $\text{IL}^{(0,1)}\text{QG}$. This speaks about stability in the $\text{IL}^{(0,1)}\text{QG}$ in high-wavenumber end of the spectrum and ensuing potentially less intense submesoscale wave activity in the nonlinear regime.
- Yet, that Arnold's method fails to demonstrate formal, let alone Lyapunov, stability for all spectrally stable states (cf. Fig. 2) suggests that the $\text{IL}^{(0,1)}\text{QG}$ may be more prone to instability than the IL^0QG , in which case all spectrally stable basic states (in a similar class) are provable Lyapunov stable [BV21b, BV24].

We back up the above inferences with the results from direct numerical simulations (cf. Appendix for numerical details) of the $\text{IL}^{(0,1)}$ and IL^0QG . These differ from those of [BV21c], which included Hamiltonian topographic forcing (cf. Section 2.6). Concretely, we considered the full nonlinear evolution of perturbations to the spectrally unstable basic state (59) defined by $\alpha = 3$, $\mu = 0$, $b = 0$, and $S = 0$, which violates (64). The initial perturbation was chosen to be a small-amplitude normal mode. Taking the zonal channel domain period (L) and width (W) to be equal to the deformation radius (R), the initial perturbation reads

$$\frac{R\delta\bar{\xi}}{U_\sigma} = -\frac{\delta\psi_\sigma}{RU_\sigma} = \frac{\delta\psi_{\sigma^2}}{RU_\sigma} = \frac{1}{2} \cos 4\pi \frac{x}{R} \sin \pi \frac{y}{R}. \quad (94)$$

For wavenumber-(2,1) $\mathbf{k} = (k, l) = (\frac{4\pi}{R}, \frac{\pi}{R})$ and the above basic state parameters, from dispersion relation (63) we compute a growth rate of $\varpi \approx 1.7 \frac{U_\sigma}{R}$ for the initial perturbation. The duration of the simulation was set to roughly $5\varpi^{-1}$, that is, five times the e-folding time of a growing normal mode. Snapshots of perturbation potential vorticity, $\delta\bar{\xi}$, at $t = 2.5\varpi^{-1}$ and $5\varpi^{-1}$ are shown in the top- and bottom-left panel of Fig. 6, respectively. Note the development of Kelvin–Helmoltz-like vortex rolls with scales much smaller than R . Initially, a scale separation is very evident. This evidence fades with time. The right panels of Fig. 6 show at corresponding times $\delta\bar{\xi}$ but in the IL^0QG . This was initialized from the same basic state as the $\text{IL}^{(0,1)}\text{QG}$ except that in the IL^0QG , $\psi_{\sigma^2} = 0$, i.e., the buoyancy is vertically uniform, so $S = 0$ and $\mu = 0$. For the parameters chosen and wavenumber-(2,1), the growth rate of the initial perturbation in the IL^0QG coincides with that in the $\text{IL}^{(0,1)}\text{QG}$. Comparing the left and right columns of Fig. 6, it is clear that submesoscale wave activity in the $\text{IL}^{(0,1)}\text{QG}$ can be more intense than, or at least as intense as, in the IL^0QG .

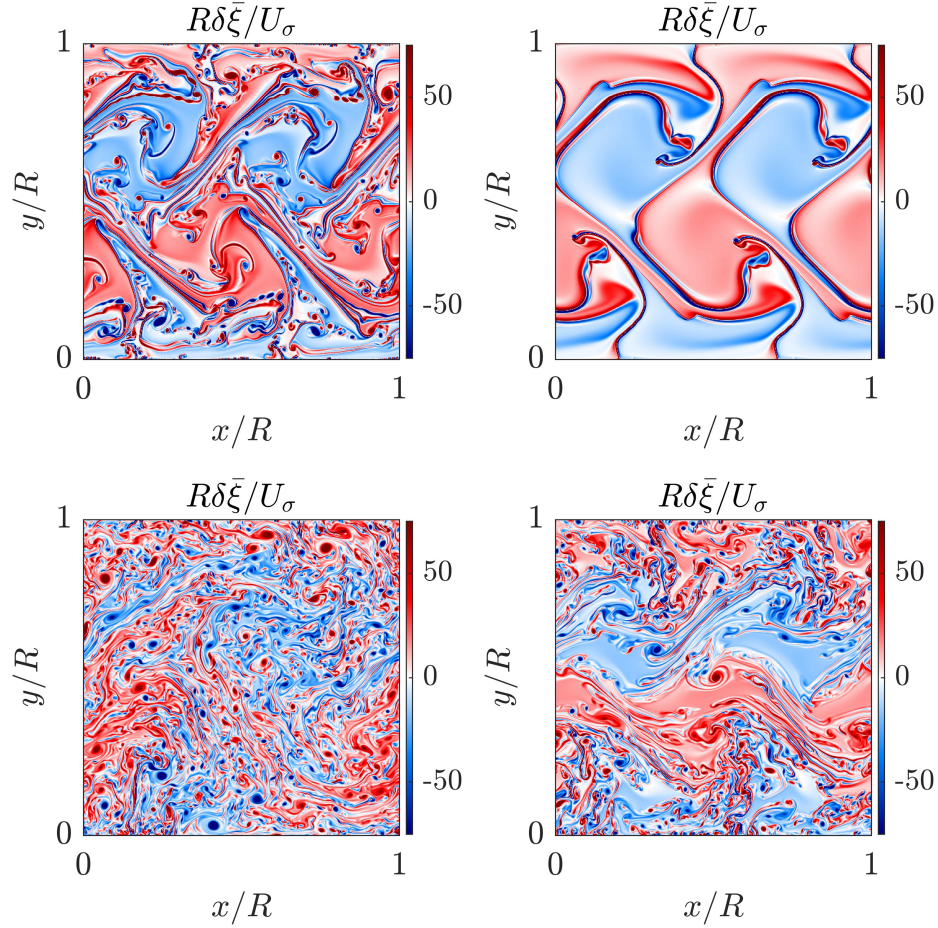


Figure 6: (left column) Snapshots at $U_\sigma t/R = 2$ (top) and 3 (bottom) of the nonlinear evolution of the potential vorticity perturbation to spectrally unstable basic state potential vorticity (59d) with $\alpha = 3$, $\mu = 0$, $b = 0$, and $S = 0$. (right column) As in the left column, but based on the IL^0QG , for which $S = 0$ and $\mu = 0$ (the buoyancy field is vertically uniform in this model).

7 Concluding remarks

In this paper, we have investigated the properties of a thermal rotating shallow-water model with uniform stratification for subinertial upper-ocean dynamics, and carried out a stability analysis in the model. The model has an active layer, limited from above by a rigid interface with the atmosphere, which freely floats atop an infinitely deep inert (abyssal) layer. The dynamics in the model is quasigeostrophic (QG). Unlike the adiabatic reduced-gravity QG model, the thermal model allows buoyancy (temperature) to vary laterally (i.e., in the

horizontal) and time. This enables the incorporation of heat and freshwater fluxes across the ocean surface. By contrast with the standard thermal model, the model considered here includes uniform stratification, still maintaining the two-dimensional structure of the thermal and adiabatic (i.e., with a homogeneous density) models. The model is a special case of a recently derived extended theory of thermal models with geometry [BV21c]. The QG version of the extended family of models is referred to as $\text{IL}^{(0,n)}\text{QG}$. Here IL stands for inhomogeneous layer. The first slot in the superscript of IL refers to the amount of vertical variation of the horizontal velocity with depth and the second one to the (whole) degree of a polynomial expansion of the buoyancy in the vertical coordinate. The particular stratified thermal QG model considered here is the $\text{IL}^{(0,1)}\text{QG}$ member of that family. The standard thermal QG model [Rip96b] is referred to as the IL^0QG , while the adiabatic QG model [Ped87] to as the HLQG.

Main findings. The $\text{IL}^{(0,1)}\text{QG}$ has unique solutions, it possess a Kelvin–Noether-like circulation theorem along material loops stating that creation (or annihilation) of circulation is due to the misalignment between the gradients of bathymetry (layer thickness) and buoyancy, and is manifestly Hamiltonian with a Lie–Poisson bracket. Geometrically, the bracket is a product for a realization Lie enveloping algebra on functionals in the dual of the extension by semidirect product of the Lie algebra of symplectic diffeomorphisms of the fluid domain, chosen here to be a periodic zonal channel of the β -plane, with two copies of the space of smooth functions on that domain. The representation of the algebra on the space of functions is given by the canonical Poisson bracket in \mathbb{R}^2 . This Hamiltonian structure is not spoiled by the addition of certain type of topographic forcing. The $\text{IL}^{(0,1)}\text{QG}$ thus preserves energy and zonal momentum, respectively related to symmetry under time shifts and zonal translations by Noether’s theorem. In addition to these conservation laws, the model has integrals of motion that form the kernel of the Lie–Poisson bracket, known as Casimirs. Unlike the usual situation in Lie–Poisson Hamiltonian systems, the $\text{IL}^{(0,1)}\text{QG}$ also supports a class of motion integrals which neither form the kernel of the bracket nor are related to any explicit symmetries of the system via Noether’s theorem. To the best of our knowledge, such integrals have so far never been reported. The model sustains the usual Rossby waves and a neutral model, both riding on a reference state, i.e., one with no currents, a special type of it being the vacuum state, i.e., one with vanishing energy. Positive definiteness of a general integral of motion, called a free energy, quadratic on the deviation from the reference state prevents perturbations of arbitrary shape and size on such a state from spuriously growing. An exception is the vacuum state, as perturbations on this state have positive-semidefinite free energy associate. Spurious growth of such perturbations cannot be prevented using free energy conservation.

The stability analysis carried out in the $\text{IL}^{(0,1)}\text{QG}$ was applied on a family of basic states representing baroclinic zonal jets with curvature in the velocity vertical profile. The $\text{IL}^{(0,1)}\text{QG}$ has velocity independent of depth. However, by the thermal-wind balance the velocity is implicitly vertically sheared. We found that a current in this family is

spectrally stable, i.e., with respect to infinitesimally small normal-mode perturbations, when the gradients of vertically averaged (mean) and layer thickness have like signs and the ratio of mean buoyancy and buoyancy frequency gradients are larger than a fraction of the reference layer thickness and vice versa. In the limit of very weak stratification, the growth rate of long perturbations, i.e., with wavelengths of the order of the equivalent barotropic Rossby deformation radius, are found to saturate. By contrast, perturbations with wavelengths of the order of the gravest Rossby radius have vanishing growth rate. Only a subset of the spectrally stable states was possible to be shown stable with respect to finite-size perturbations of arbitrary structure using the integrals of motion by means of the application of Arnold’s method. These integrals exclude the newly found ones, whose role in constraining stratified thermal flow remains to be understood. The states shown stable using Arnold’s method are of Lyapunov type, i.e., the instantaneous perturbation distance to such states as measured using an L^2 norm is bounded at all times by a multiple of the initial distance to them. These Lyapunov-stable states were used to a-priori bound the nonlinear growth of perturbations to spectrally unstable states, thereby preventing evolution in the $\text{IL}^{(0,1)}\text{QG}$ from undergoing an ultraviolet explosion. This is extensible to perturbations to any unstable state, including the vacuum state, whose free energy can be vanishing.

Our findings do not support the generality of earlier numerical evidence suggesting that suppression of sub-deformation scale (i.e., submesoscale) wave activity is a result of the inclusion of stratification in thermal shallow-water theory. We backed up the latter with results of direct, fully nonlinear simulations of the $\text{IL}^{(0,1)}\text{QG}$ and IL^0QG , which did not include topographic forcing as previously considered.

Outlook. Left for future work is finding the origin of the non-Casimir integrals of motion in the $\text{IL}^{(0,1)}\text{QG}$. Preliminary work using the primitive-equation parent model [BV21c] suggests that these conservation laws are related via Noether’s theorem, just as Casimirs are, to invariance of the Eulerian variables under relabeling of fluid particles. Also left for the future is the implementation of structure preserving algorithms to more accurately frame numerically fully nonlinear evolution in the $\text{IL}^{(0,1)}\text{QG}$ compared to that in the IL^0QG . This should be done in connection to the nature of turbulence in these models, which is different than that in the HLQG for not being constrained by enstrophy conservation, and how this relates to observations. One obstacle to overcome is the development of a geometric (Lie–Poisson) integrator for flows on the annulus, of interest here, as these currently exist only on the torus or the sphere (e.g., [MV19, CVL⁺22]).

Acknowledgements

We thank Phil Morrison for calling our attention to vacuum states. We owe Darryl Holm our renewed interest in thermal fluids, originally introduced to us by the late Pedro Ripa

while being graduate students of Departamento de Oceanografía Física of CICESE (Ensenada, Baja California, Mexico) under his direction.

Appendix: Numerical details of the direct simulations

The numerical simulation of the $IL^{(0,1)}QG$ employed a pseudospectral scheme with fast Fourier transform (FFT) in x and discrete sine transform (DST) in y to invert (4d), but as written for the *perturbation* to the (unstable) basic state. We consistently wrote the entire set (4) accordingly. The DST imposes a homogeneous Dirichlet boundary condition on $\delta\bar{\psi}$ without spoiling the strict zero-normal-flow at the channel northern and southern walls boundary conditions, namely, $\partial_x\bar{\psi}|_{y=0,W} = 0$. A total of 512 grid points in each direction, zonal and meridional, was considered. Differentiation was done using dialiased FFT in each direction using the $\frac{3}{2}$ zero-padding rule (we tried Chebyshev differentiation in y , but this led to numerical instability). The equations were forward advanced using a fourth-order Runge–Kutta method with time step $\Delta t U_\sigma / R \approx 0.0001$ as resulting by applying the Courant–Friedrichs–Lewy condition. Finally, a small amount (roughly $-1.5 \times 10^{-11} U_\sigma R^3$) of biharmonic hyperviscosity was included to stabilize the time step. The same numerical treatment was applied to the simulation of the IL^0QG . Our confidence on the simulations is measured by how well the conservation laws in the $IL^{(0,1)}QG$ and IL^0QG are represented. Take energy (\mathcal{E}), momentum (\mathcal{M}), and two Casimirs common to the $IL^{(0,1)}QG$ and IL^0QG , e.g., $\mathcal{C}_{1,0}$ and $\mathcal{C}_{1,\cos\psi_\sigma}$; cf. (43) and (47). The absolute magnitude of the relative error with respect to the values of these quantities initially are about 19.2, 2.6, 2.8, and 2.9% for the $IL^{(0,1)}QG$, and 17.3, 12.2, 3.0, and 3.3% for the IL^0QG .

References

- [ACBVG⁺22] Feranando Andrade-Canto, Francisco J. Beron-Vera, Gustavo J. Goni, Daniel Karrasch, Maria J. Olascoaga, and Joquin Trinanes. Carriers of *Sargassum* and mechanism for coastal inundation in the Caribbean Sea. *Phys. Fluids*, 34:016602, 2022.
- [Arn14] Vladimir I. Arnold. *Vladimir I. Arnold - Collected Works: Hydrodynamics, Bifurcation Theory, and Algebraic Geometry 1965-1972*. Springer Berlin Heidelberg, 2014.
- [Bei97] E. Beier. A numerical investigation of the annual variability in the Gulf of California. *J. Phys. Oceanogr.*, 27:615–632, 1997.
- [Ben84] T.B. Benjamin. Impulse, flow force and variational principles. *IMA J. Appl. Math.*, 32:3–68, 1984.
- [BFF07] G. Boccaletti, R. Ferrari, and B. Fox-Kemper. Mixed layer instabilities and restratification. *J. Phys. Oceanogr.*, 37:2228–2250, 2007.

- [BV21a] F. J. Beron-Vera. Multilayer shallow-water model with stratification and shear. *Rev. Mex. Fis.*, 67:351–364, 2021.
- [BV21b] F. J. Beron-Vera. Nonlinear saturation of thermal instabilities. *Phys. Fluids*, 33:036608, 2021.
- [BV21c] Francisco J. Beron-Vera. Extended shallow-water theories with thermodynamics and geometry. *Phys. Fluids*, 33:106605, 2021.
- [BV24] F. J. Beron-Vera. On a priori bounding the growth of thermal instability waves. *Phys. Fluids*, in press (doi:10.48550/arXiv.2402.13002), 2024.
- [CH12] C. J. Cotter and D. D. Holm. On Noether’s theorem for the Euler–Poincaré equation on the diffeomorphism group with advected quantities. *Foundations of Computational Mathematics*, 13:457–477, 2012.
- [CHL⁺23] D. Crisan, D. D. Holm, E. Luesink, P. R. Mensah, and W. Pan. Theoretical and computational analysis of the thermal quasi-geostrophic model. *Journal of Nonlinear Science*, 33(5):96, 2023.
- [CKLZ23] Yangyang Cao, Alexander Kurganov, Yongle Liu, and Vladimir Zeitlin. Flux globalization based well-balanced path-conservative central-upwind scheme for two-layer thermal rotating shallow water equations. *Journal of Computational Physics*, 474:111790, 2023.
- [CVL⁺22] Paolo Cifani, Milo Viviani, Erwin Luesink, Klas Modin, and Bernard J. Geurts. Casimir preserving spectrum of two-dimensional turbulence. *Phys. Rev. Fluids*, 7:L082601, 2022.
- [Del03] P. J. Dellar. Common Hamiltonian structure of the shallow water equations with horizontal temperature gradients and magnetic fields. *Phys. Fluids*, 15:292–297, 2003.
- [EDK19] Christopher Eldred, Thomas Dubos, and Evaggelos Kritsikis. A quasi-Hamiltonian discretization of the thermal shallow water equations. *Journal of Computational Physics*, 379:1–31, 2019.
- [FjØ50] R. Fjørtoft. Application of integral theorems in deriving criteria of stability for laminar flows and for the baroclinic circular vortex. *Geofys. Publ.*, 17:1–52, 1950.
- [FMP95] Y. Fukamachi, J. P. McCreary, and J. A. Proehl. Instability of density fronts in layer and continuously stratified models. *J. Geophys. Res.*, 100:2559–2577, 1995.
- [GLZD17] E. Gouzien, N. Lahaye, V. Zeitlin, and T. Dubos. Thermal instability in rotating shallow water with horizontal temperature/density gradients. *Physics of Fluids*, 29:101702, 2017.
- [HHS22] Darryl D. Holm, Ruihao Hu, and Oliver D. Street. *Coupling of Waves to Sea Surface Currents Via Horizontal Density Gradients*, page 109–133. Springer International Publishing, 2022.
- [HL21] D. D. Holm and E. Luesink. Stochastic wave–current interaction in thermal shallow water dynamics. *J. Nonlinear Sci.*, 31:29, 2021.

- [HLP21] Darryl D. Holm, Erwin Luesink, and Wei Pan. Stochastic mesoscale circulation dynamics in the thermal ocean. *Phys. Fluids*, 33:046603, 2021.
- [HMR02] D. D. Holm, J. E. Marsden, and T. S. Ratiu. The Euler-Poincaré equations in geophysical fluid dynamics. In J. Norbury and I. Roulstone, editors, *Large-Scale Atmosphere-Ocean Dynamics II: Geometric Methods and Models*, pages 251–299. Cambridge University, 2002.
- [HMRW85] D. D. Holm, J. E. Marsden, T. Ratiu, and A. Weinstein. Nonlinear stability of fluid and plasma equilibria. *Phys. Rep.*, 123:1–116, 1985.
- [Hol15] Darryl D. Holm. Ideal shallow water dynamics in a rotating frame. MPE CDT PDE Lecture Notes, 2015.
- [KLZ20] Alexander Kurganov, Yongle Liu, and Vladimir Zeitlin. Moist-convective thermal rotating shallow water model. *Physics of Fluids*, 32:066601, 2020.
- [KO58] M. D. Kruskal and C. Oberman. Stability of plasma in static equilibrium. *Phys. Fluids*, 1:275, 1958.
- [LMM86] D. Lewis, J. Marsden, and R. Montgomery. The Hamiltonian structure for dynamic free boundary problem. *Physica D*, 18:391–404, 1986.
- [LZD20] Noe Lahaye, Vladimir Zeitlin, and Thomas Dubos. Coherent dipoles in a mixed layer with variable buoyancy: Theory compared to observations. *Ocean Modelling*, 153:101673, 2020.
- [Mah16] A. Mahadevan. The impact of submesoscale physics on primary productivity of plankton. *Annu. Rev. Mar. Sci.*, 8:161–184, 2016.
- [McG16] Dennis J. McGillicuddy. Mechanisms of physical-biological-biogeochemical interaction at the oceanic mesoscale. *Annual Review of Marine Science*, 8:125–159, 2016.
- [McW16] J. C. McWilliams. Submesoscale currents in the ocean. *Proc R Soc A*, 472:20160117, 2016.
- [ME86] P. J. Morrison and S. Eliezer. Spontaneous symmetry breaking and neutral stability in the noncanonical hamiltonian formalism. *Physical Review A*, 33:4205–4214, 1986.
- [MG80] P. J. Morrison and J. M. Greene. Noncanonical Hamiltonian density formulation of hydrodynamics and ideal magnetohydrodynamics. *Phys. Rev. Lett.*, 45:790–794, 1980.
- [MH84] P. J. Morrison and R. D. Hazeltine. Hamiltonian formulation of reduced magnetohydrodynamics. *Phys. Fluids*, 27:886–897, 1984.
- [MK88] J. P. McCreary and P.K. Kundu. A numerical investigation of the Somali current during the southwest monsoon. *J. Mar. Res.*, 46:25–58, 1988.
- [Mor98] P. J. Morrison. Hamiltonian description of the ideal fluid. *Rev. Mod. Phys.*, 70:467–521, 1998.
- [MRW84] Jerrold E. Marsden, Tudor Ratiu, and Alan Weinstein. Semidirect products and reduction in mechanics. *Transactions of the American Mathematical Society*, 281(1):147–177, 1984.

- [MS87] M. E. McIntyre and T. G. Shepherd. An exact local conservation theorem for finite-amplitude disturbances to non-parallel shear flows, with remarks on hamiltonian structure and on arnol'd's stability theorems. *Journal of Fluid Mechanics*, 181:527, 1987.
- [MV19] Klas Modin and Milo Viviani. A Casimir preserving scheme for long-time simulation of spherical ideal hydrodynamics. *Journal of Fluid Mechanics*, 884:A22, 2019.
- [OR67] J. J. O'Brien and R. O. Reid. The non-linear response of a two-layer, baroclinic ocean to a stationary, axially-symmetric hurricane: Part I: Upwelling induced by momentum transfer. *J. Atmos. Sci.*, 24:197–207, 1967.
- [OSP98] J. L. Ochoa, J. Sheinbaum, and E. G. Pavía. Inhomogeneous rodons. *J. Geophys. Res.*, 103:24869–24880, 1998.
- [Ped82] J. Pedlosky. Finite-amplitude baroclinic waves at minimum critical shear. *J. Atmos. Sci.*, 39:555–562, 1982.
- [Ped87] J. Pedlosky. *Geophysical Fluid Dynamics*. Springer, 2nd edition, 1987.
- [PP00] R. Pinet and E. Pavía. Stability of elliptical horizontally inhomogeneous rodons. *J. Fluid Mech.*, 416:29–43, 2000.
- [Rip83] P. Ripa. General stability conditions for zonal flows in a one-layer model on the beta-plane or the sphere. *J. Fluid Mech.*, 126:463–487 (received May 1982 and revised Aug 1982), 1983.
- [Rip92] P. Ripa. Sistemas Hamiltonianos singulares. I: Planteamiento del caso discreto, Teorema de Noether. *Rev. Mex. Fís.*, 38:984–1004, 1992.
- [Rip93a] P. Ripa. Arnol'd's second stability theorem for the equivalent barotropic model. *J. Fluid Mech.*, 257:597–605, 1993.
- [Rip93b] P. Ripa. Conservation laws for primitive equations models with inhomogeneous layers. *Geophys. Astrophys. Fluid Dyn.*, 70:85–111, 1993.
- [Rip95] P. Ripa. On improving a one-layer ocean model with thermodynamics. *J. Fluid Mech.*, 303:169–201, 1995.
- [Rip96a] P. Ripa. Linear waves in a one-layer ocean model with thermodynamics. *J. Geophys. Res. C*, 101:1233–1245, 1996.
- [Rip96b] P. Ripa. Low frequency approximation of a vertically integrated ocean model with thermodynamics. *Rev. Mex. Fís.*, 42:117–135, 1996.
- [Rip99] P. Ripa. On the validity of layered models of ocean dynamics and thermodynamics with reduced vertical resolution. *Dyn. Atmos. Oceans*, 29:1–40, 1999.
- [Rip00] P. Ripa. Estabilidad e inestabilidad. Parte i: Uso de integrales de movimiento en el problema de estabilidad. *Rev. Mex. Fís.*, 42:413–518, 2000.
- [SC83] P.S. Schopf and M.A. Cane. On equatorial dynamics, mixed layer physics and sea surface temperature. *J. Phys. Oceanogr.*, 13:917–935, 1983.
- [She88] T.G. Shepherd. Rigorous bounds on the nonlinear saturation of instabilities

- to parallel shear flows. *J. Fluid Mech.*, 196:291–322, 1988.
- [WD13] E. S. Warneford and P. J. Dellar. The quasi-geostrophic theory of the thermal shallow water equations. *J. Fluid Mech.*, 723:374–403, 2013.